agronomy

MDPI

Article

Identification of HIR, EDS1 and PAD4 Genes Reveals Differences between *Coffea* Species That May Impact Disease Resistance

Sílvia Tavares [1,2,3], Helena Azinheira [1,2,*], Javier Valverde [4,5], A. Jesus Muñoz-Pajares [4,6], Pedro Talhinhas [2] and Maria do Céu Silva [1,2]

1 CIFC—Centro de Investigação das Ferrugens do Cafeeiro, Instituto Superior de Agronomia, Universidade de Lisboa, Quinta do Marquês, 2784-505 Oeiras, Portugal; satavares@isa.ulisboa.pt (S.T.)
2 LEAF—Linking Landscape, Environment, Agriculture and Food Research Center, Associated Laboratory TERRA, Instituto Superior de Agronomia, Universidade de Lisboa, Tapada da Ajuda, 1349-017 Lisboa, Portugal; ptalhinhas@isa.ulisboa.pt
3 Department of Plant and Environmental Sciences, Copenhagen Plant Science Center, University of Copenhagen, 1871 Frederiksberg C, Denmark
4 CIBIO, InBIO—Research Network in Biodiversity and Evolutionary Biology, University of Porto, Campus Agrário de Vairão, 4485-661 Vairão, Portugal; javi.val.mor@gmail.com (J.V.); ajesusmp@go.ugr.es (A.J.M.-P.)
5 Estación Biológica de Doñana, Consejo Superior de Investigaciones Científicas (CSIC), Avenida Américo Vespucio 26, Isla de La Cartuja, 41092 Sevilla, Spain
6 Department of Genetics, Faculty of Sciences, University of Granada, 18071 Granada, Spain
* Correspondence: hmga@edu.ulisboa.pt

Abstract: Coffee, a widely consumed important agricultural product, is mainly produced from two species, *Coffea arabica* (Arabica coffee) and *C. canephora* (Robusta coffee). Timor Hybrid (HDT) is a population resulting from a natural cross between *C. arabica* and *C. canephora*. HDT derivatives have a high spectrum of resistance to different races of *Hemileia vastatrix* (Hv), the causal agent of coffee leaf rust. A RNAseq database, obtained from HDT832/2 leaves inoculated with Hv (Host Resistance) and *Uromyces vignae* (Uv, Nonhost Resistance), showed the presence of genes implicated in the hypersensitive response and salicylic acid pathway. Hypersensitive Induced Reaction (HIR) gene family, Enhanced Disease Susceptibility1 gene (EDS1), and Phytoalexin Deficient 4 (PAD4) gene are involved in host and nonhost resistance. Relative expression calculated by RT-qPCR was used to confirm and expand the transcriptome analysis. *HDTHIR4*, *HDTEDS1*, and *HDTPAD4* showed the highest upregulation in response to Hv and Uv inoculation, confirming a similar trend in host and nonhost resistance in HDT. HIR and EDS1/PAD4 gene families were characterized for the first time in the three available *Coffea* genomes. HIR genes were quite conserved between *Coffea* species. Surprisingly, EDS1 and PAD4 genes revealed major differences in gene structure. The PAD4 predicted protein from *C. arabica* does not include both conserved domains of the EDS1/PAD4 family, and the EDS1 putative protein from *C. canephora* includes a formin domain unusual in the same protein family. The variability shown by EDS1/PAD4 gene family may impact the disease resistance response of *Coffea* species, which can be surveyed for the gene sequences that will produce a more resistant phenotype.

Keywords: *Coffea* spp.; basal resistance; EDS1; HIR; PAD4; coffee leaf rust; Timor hybrid

Citation: Tavares, S.; Azinheira, H.; Valverde, J.; Muñoz-Pajares, A.J.; Talhinhas, P.; Silva, M.d.C. Identification of HIR, EDS1 and PAD4 Genes Reveals Differences between *Coffea* Species That May Impact Disease Resistance. *Agronomy* **2023**, *13*, 992. https://doi.org/10.3390/agronomy13040992

Academic Editor: Danyu Shen

Received: 21 December 2022
Revised: 16 March 2023
Accepted: 21 March 2023
Published: 28 March 2023

1. Introduction

Coffee is one of the most valuable commodities in the world, second to oil in transactable value [1]. In 1861, Coffee Leaf Rust (CLR) was identified for the first time in East Africa. Afterward, CLR spread to all coffee-growing countries, including Ceylon (now Sri Lanka), in 1869, where it caused the first serious CLR outbreak leading to the eradication

of coffee production in this country, which had devastating social and economic consequences [2] and references therein. However, from the 1970s on, CLR was considered a manageable disease mainly controlled by fungicide application or by planting resistant varieties. In the second decade of the 21st century, Central and South America saw a resurgence of CLR attributed to inadequate agricultural practices and climate change [3]. In 2019 the decline in coffee prices and the increase in production costs, namely in the price of fungicides, made the situation even worse, causing a severe social crisis in Central American countries that led to population migration due to economic anxiety [4].

CLR is caused by *Hemileia vastatrix*, a basidiomycete obligate parasite of coffee plants. The infection process starts with the germination of *H. vastatrix*'s urediniospores on coffee leaves and culminates in a compatible interaction with the production of new urediniospores bursting through the stomatal aperture. In incompatible interactions, the fungal growth is halted before or after the formation of haustoria, named pre- or post-haustorial resistance, respectively [2]. The interaction between *Coffea* and *H. vastatrix* is ruled by the gene-for-gene theory. At least nine dominant genes (S_H1–S_H9), combined or alone, are involved in the resistance, and nine concomitant virulence genes were described in coffee rust (*v1*–*v9*) [5].

At the beginning of the 20th century, on the island of Timor, a natural hybrid between *Coffea arabica* and *C. canephora* was discovered to be resistant to CLR. This population, named Timor Hybrid (HDT), was subsequently backcrossed to *C. arabica.* Several accessions of HDTs were used as sources of resistance to CLR in coffee breeding programs [6]. HDTs resistance to *H. vastatrix* is conferred by the *C. canephora* parent-derived genes, namely S_H6, S_H7, S_H8, S_H9, and others not yet identified [5].

From all the HDTs genotypes, HDT832/2 depicts a stronger and more durable resistance to most *H. vastatrix* races. This resistance is characterized by a visible hypersensitive-like response (HR) and accumulation of phenolic compounds, accompanied by an increase in the transcription level of genes involved in the salicylic acid pathway [7], which results in a strong capacity for basal resistance and a pre-haustorial resistance resembling a *Coffea* nonhost-like response [7,8].

Plants rely on a layered response to fend off pathogens. One of the layers is composed of conserved membrane receptors able to recognize pathogen molecules (pathogen-associated, PAMPs) or plant molecules (damage-associated, DAMPs) [9]. Plants counteract with another layer of defense that relies on cytoplasmic receptors from the family of intracellular nucleotide-binding leucine-rich repeat proteins (NLRs) that recognize avirulent pathogen effectors. Cell death linked to HR is a hallmark in the process of effector recognition by NLRs [10]. HR can also occur in nonhost interactions suggesting that some NLRs can also be involved, which is consistent with recent research showing that host and nonhost resistance fundamentally rely on similar genes and pathways [11].

The *Hypersensitive Induced Reaction* (*HIR*) gene family encodes proteins containing the stomatin/prohibitin/flotillin/HflK (SPFH) domain, also named the prohibitin domain or band seven domain [12]. The first plant HIR protein studied was isolated from tobacco (NG1). HR-like symptoms were observed together with the induction of pathogen-related protein 2 (PR2) when the *NG1* gene was overexpressed in tobacco plants infected with a Tobacco Mosaic Virus (TMV) vector [13]. Since then, NG1 homologous have been identified in other plant species, both monocots and dicots. However, the molecular mechanism employed by HIR proteins is largely unknown [12].

HIR genes were found to be transcriptionally activated in response to PAMPs [12] induced by viruses, bacteria, and fungi, including rusts [14,15]. In barley, lesion mimic mutants that undergo spontaneous cell death are related to HR [16]. Their overexpression in *Nicotiana benthamiana*, besides triggering HR, led to the accumulation of salicylic acid (SA), which was impaired in *eds1* (*Enhanced Disease Susceptibility 1*) mutant plants, linking HIR action to the *EDS1* gene regulatory node [17]. The *EDS1* gene is involved in numerous processes related to plant resistance and has a central role in basal resistance to biotrophic pathogens together with *PAD4* (*Phytoalexin Deficient 4*) gene [18].

EDS1, PAD4, and SAG101 (*Senescence Associated Gene 101*) are one protein family unique to plants. The three proteins share two specific protein domains, one exclusive to plants named EP and another at the N-terminus, similar to eukaryotic lipases [18]. EDS1, associated with PAD4, was found to be essential in basal immune response and production of SA [19]. Moreover, EDS1 by itself is an important component in effector-triggered immunity (ETI) in the signaling cascade generated by intercellular Toll/interleukin-1 NLRs receptors (TNLs). EDS1 protein, as a homodimer or as a heterocomplex with PAD4 and SAG101 proteins, acts as a regulatory node in response to biotic stress [18–20].

To understand better the transcript profile associated with HDT832/2 resistance to CLR and to detect common and distinct responses of a nonhost response from a non-adapted rust pathogen (*Uromyces vignae*), we analyzed a RNAseq database from HDT832/2 leaves. The data highlighted genes connected with HR and SA processes. In this context, *HIR*, *EDS1,* and *PAD4* gene families were chosen as representatives of both responses. The chosen genes showed somewhat distinct transcription profiles; the *PAD4* gene was present in inoculated and control leaves; likewise, several genes from the HIR family and the *EDS1* gene were only expressed in data from inoculated leaves. A RT-qPCR analysis confirmed the presence of all genes in inoculated leaves and widened the analysis to the transcript profile in order to include a complete picture of the infection process. The release of *C. arabica* (https://www.ncbi.nlm.nih.gov/assembly/GCF_003713225.1, accessed on 1 October 2022), *C. canephora* (http://www.coffee-genome.org/coffeacanephora, accessed on 1 October 2022) [21] and *C. eugenioides* (https://www.ncbi.nlm.nih.gov/assembly/GCF_003713205.1, accessed on 1 October 2022) genomes permitted us to analyze for the first time all the three gene families in *Coffea* genomes and compare them with the transcript sequences obtained from HDT transcriptome. Our analysis shows significant variability in the gene structure and protein sequence of EDS1 and PAD4 in *Coffea* species that may impact the resistance response exhibited by each species.

2. Materials and Methods

2.1. Coffee Plants, Rust Isolates, Growth and Inoculation Conditions

Coffee plants were maintained in pots in greenhouse conditions under temperatures ranging from 15 to 30 °C. The inoculation experiments were conducted under the same conditions, and two and three independent biological experiments were used for the RT-qPCR analysis.

HDT genotype CIFC HDT832/2 was inoculated with *H. vastatrix* CIFC isolate 1065 (race II, virulence gene v_5) and *Uromyces vignae* isolate CPR-1 (race I) to establish host incompatible and nonhost interactions, respectively. Mock-inoculated leaves were used as controls. Four *C. arabica* genotypes, var. Caturra (CIFC 19/1), CIFC H147/1, CIFC 128/2, and CIFC H469/16 were inoculated with *H. vastatrix* CIFC isolate 178a (race XIV, virulence genes $v_{2,3,4,5}$). The first two genotypes established a compatible interaction with isolate 178a, and last ones had an incompatible interaction with 178a.

The inoculation procedure is described in full detail by Diniz et al. [7]. Briefly, young fully expanded leaves (10 to 12 days old) located at the terminal node were inoculated with *H. vastatrix* or *U. vignae* urediniospores (1 mg per pair of leaves). The spores were placed with a scalpel on the lower surface of coffee leaves and gently spread with a camel-hair brush. *U. vignae* urediniospores were previously washed with 0.01% (*v*/*v*) Tween 20 for 30 s at room temperature (24 °C). Inoculated leaves were sprayed with distilled water, and the plants placed for 24 h under darkness in moist chambers, after which were transferred to greenhouse conditions.

2.2. Light Microscope Observation of Fresh Tissues

Spore germination and appressoria formation over stomata was evaluated at the microscope as described in [22]. Leaves with a germination rate above 50% were used for evaluating rust post-penetration structures, which were accounted in cross sections ob-

tained from leaf fragments cut at a freezing microtome (Leica CM1850; Zurich, Switzerland), stained with blue lactophenol and observed at the microscope [23,24].

In order to detect autofluorescent cells, cross sections were placed in 0.07 M pH 8.9 phosphate solution (K_2HPO_4) for 5 min and mounted in the same solution [23]. Autofluorescence under epifluorescence blue light is thought to indicate the presence of phenolic-like compounds and cytoplasmatic autofluorescence in cytoplasm and/or browning frequently associated with plant cell death [7,24].

Observations were made with a light microscope Leica (Zurich, Switzerland) DM-2500 equipped with a mercury bulb HB 100 W, u.v. light (excitation filter BP 340–380; barrier filter LP 430) and blue light (excitation filter BP 450–490; barrier filter LP 515), Leica (Zurich, Switzerland).

2.3. RNA Isolation, cDNA Synthesis for Pyrosequencing and Reads Assembly

Coffee leaves of HDT 832/2 inoculated with *H. vastatrix* (pooled sample H) or with *U. vignae* (pooled sample U) were harvested 21 and 24 h after inoculation (hai) or 9 and 12 hai, respectively. The control (pooled sample C) was composed of uninoculated leaves kept for 9, 12, 21, and 24 hai under similar incubation conditions as the inoculated samples. Pooled samples were established after RNA extraction by combining 500 ng of RNA from individual samples.

Total RNA was extracted from frozen coffee leaf samples using the RNeasy Plant Mini kit (Qiagen, Hilden, Germany), with addition of an in-column DNase I digestion, according to Appendix E of the RNeasy Plant Mini kit manual. RNA samples after DNase I digestion with high purity were used for cDNA synthesis. The quality and concentration of RNA samples were assessed by capillary electrophoresis (Agilent 2100 Bioanalyzer, Agilent Technologies, Santa Clara, CA, USA). A control PCR with cytochrome b gene primers was run on extracted RNA samples to check for contamination with genomic DNA.

First-strand cDNA was synthesized using the SMARTer Pico PCR cDNA Synthesis Kit (Clonetech, USA), the 3′ SMART CDS Primer II A, and SMARTScribe Reverse Transcriptase (as detailed in the kit manual). cDNA was amplified with 20 amplification cycles using 5′ PCR Primer II A and Advantage 2 Polymerase Mix (as detailed in the kit manual). Amplified cDNA was purified using the Nucleospin Extract II kit (Macherey-Nagel, Düren, Germany) and evaluated by 1.2% agarose gel electrophoresis and spectrophotometry (Nanodrop 2000, Thermo Scientific, Waltham, MA, USA). A total of 20 µg cDNA (approximately 200 ng/µL) for each pooled sample was sent for 454 pyrosequencing (Genome Sequencer FLX Titanium System) at Beckman Coulter Genomics (Indianapolis, USA). The assembly of the 877,790 pyrosequencing reads was performed using the Roche Newbler 2.5 (Roche) assembler following recommended parameters provided by Roche. The relative abundance (Ra) of transcripts was calculated as the ratio between the number of 454 reads per contig and the length of the assembled contig [25].

2.4. Primer Design and Standard Molecular Biology Techniques

The Clone Manager 5 software (S&E Software, USA) was used for primer design and for the analysis of sequence data from PCR products. A list of primers used is included as a supplementary file (File S1). Standard molecular biology technologies, such as PCR and PCR product purification, were performed as described in Sambrook & Russell [26] according to good laboratory practices standards.

2.5. RNA Isolation and cDNA Synthesis for RT-qPCR Analysis

RNA was isolated and quantified as described in Section 2.3. RNA quality was assessed by electrophoresis on 1.2% agarose gels. Genomic contamination in RNA extractions was checked in a control qPCR with primers for reference genes. First-strand cDNA was synthesized from 1 µg of total RNA in 20 µL final volume, using Omniscript RT kit (Qiagen) and oligo(dT)18 primer (Thermo Scientific) following manufacturer's instructions. qPCR was performed on an iQ5 thermocycler (BioRad, Hercules, CA, USA) using EvaGreen Supermix (Bio-

Rad). Each reaction comprised 1/10 dilution of the cDNA reaction, 0.5× EvaGreen Supermix, 0.3 µM of each primer, and sterile distilled water. A two-step qPCR program was chosen; initial denaturation step at 95 °C for 10 min, followed by 45 cycles of 95 °C for 15 s and 60 °C for 30 s. A melting curve analysis ranging from 60 to 95 °C was performed at the end of the qPCR cycles, with increasing temperature in a stepwise fashion by 0.5 °C every 10 s. Each PCR reaction was performed in duplicate, and amplicon specificity was checked by melting curve analysis and a 3% agarose gel electrophoresis.

Three genes depicting constant transcript levels in C, H, and U samples were chosen for qPCR normalization: Actin-11, Polyubiquitin-like, and Tubulin alpha-2 chain. The web interface RefFinder was used to evaluate their stability as reference genes (https://www.heartcure.com.au/reffinder/?type=reference) (accessed on 12 July 2022) [27]. RefFinder combines GeNorm, NormFinder, and BestKeeper software programs and ranks the best candidate for each experimental condition. qPCR primer efficiency was evaluated in a dilution curve and quantified by LinRegPCR v11.0 software (http://LinRegPCR.nl) (accessed on 12 October 2022) [28].

The relative quantification of *HIR*, *EDS1*, and *PAD4* genes was calculated using the method developed by Pfaffl (2001) [29]:

$$\text{Fold change} = \frac{\left(E_{target}\right)^{\Delta Ct,\ target(calibrator-test)}}{\sqrt[n]{E_{ref1}{}^{-\Delta Ct,\ target(calibrator-test)} \times E_{ref2}{}^{-\Delta Ct,\ target(calibrator-test)} \times E_{ref3}{}^{-\Delta Ct,\ target(calibrator-test)}}} \quad (1)$$

E—primer efficiency, *Ct*—quantification cycle.

2.6. Identification of HIR, EDS1 and PAD4 Genes in Coffea Arabica, Coffea Canephora and Coffea Eugenioides Genome Databases and Chromosome Localization

HDT sequences were used as query in the BLAST engine to identify *HIR*, *EDS1* and *PAD4* genes in fully sequenced genomes of *C. arabica* (https://www.ncbi.nlm.nih.gov/assembly/GCF_003713225.1) (accessed on 3 October 2022) and *C. eugenioides* (https://www.ncbi.nlm.nih.gov/assembly/GCF_003713205.1) (accessed on 3 October 2022) at NCBI, and *C. canephora* (http://coffee-genome.org/blast) (accessed on 3 October 2022) at Coffee genome hub. Chromosome localization was conducted on the same genome platforms.

2.7. DNA and Protein Sequence Analyses

Exon–intron organization was predicted by alignment of DNA and mRNA sequences using Clone Manager 5 software (S&E Software, USA). DNA, mRNA, and Protein sequences were aligned using the T-Coffee server (https://tcoffee.crg.eu) (accessed on 16 November 2022) [30] and visualized with the pyBoxShade program (https://github.com/mdbaron42/pyBoxshade) (accessed on 20 March 2023).

In silico analysis of conserved protein domains was carried out at NCBI using BLASTp engine (http://www.ncbi.nlm.nih.gov/Structure/cdd/cdd.shtml) (accessed on 7 October 2022) as described by Marchler-Bauer et al. [31]. PROSITE at ExPaSy server was used to scan the sequences for conserved motifs (http://www.expasy.ch/tools/scanprosite/) (accessed on 10 October 2022). Transmembrane domains were predicted at TMHMM (http://www.cbs.dtu.dk/services/TMHMM/) (accessed on 10 October 2022) and Phobius (https://phobius.sbc.su.se) (accessed on 13 October 2022) [32] servers, and myristoylation sites at ExPaSy (https://web.expasy.org/myristoylator/) (accessed on 17 October 2022). MEME (Motif-based sequence analysis) tool (https://meme-suite.org/meme/) (accessed on 18 October 2022) [33] was used to detect new conserved motifs in HIR proteins.

2.8. Phylogenetic Analysis

Phylogenetic analysis was performed by using the Maximum Likelihood method based on the JTT matrix-based model [34], conducted in MEGA7 [35].

2.9. Analysis of the Genomic Structure of PAD4 Gene in Coffea Arabica Genotypes

The genomic structure of PAD4 gene in selected *C. arabica* genotypes, CIFC 19/1, CIFC H147/1, CIFC 128/2 and CIFC 469/16, was investigated for similarities with the genomic structure of *C. canephora* and *C. eugenioides*. To do so, we used paired-end reads of 150 bp with insert sizes of approximately 500 bp from whole-genome sequencing of each genotype. Reads were trimmed to eliminate low-quality ends at a quality threshold of 20 using cutadapt v. 1.15 [36]. Trimmed reads were then mapped using the Burrows–Wheeler Aligner software [37] on a fasta file containing two contigs of 15,000 bp corresponding to the regions in the genomes of *C. canephora* and *C. eugenioides* spanning the PAD4 gene. We then filtered the mapped reads and kept those with a mapping quality (*q*) above 20, calculated as $-10 \times \log10$ Pr (mapping position is wrong), and obtained the following information: (a) percentage of paired reads with both ends mapped on the same contig; (b) mapping quality; and (c) distance between paired reads.

2.10. Statistical Analyses

The qPCR data were analyzed by two-way ANOVA followed by the Tukey test when the *p*-values were lower than 0.05 using the SigmaPlot software (SigmaPlot, Systat Software Incorporation, CA, USA). Time post-inoculation and treatment (control and infected) were treated as two independent variables.

3. Results

3.1. Transcriptome Analysis of HDT Leaves Inoculated with Hemileia vastatrix and Uromyces vignae

The transcriptome was constituted by cDNA sequences expressed in leaves of HDT inoculated with *H. vastatrix* (database H) and *U. vignae* (database U) and control (mock-inoculated) (database C). The reads analyses ensured a high-quality assembly of equal sequences, secured longer sequences, fused duplicate sequences, and subtracted low-quality reads. The sequences were annotated using BLASTn and GO terms analyses and mapped initially onto the *C. canephora* genome [21] and later on to *C. arabica* and to *C. eugenioides* genomes.

Overall, the qualitative analysis of the transcriptome data in response to inoculation with both rust species showed a high number of ESTs connected with the SA pathway and HR. Two gene families were chosen for in-depth analysis: *HIR* genes based on their involvement in HR and expression as a gene family and *EDS1/PAD4* genes due to their diverse role in plant immunity and connection to *HIR* genes [17]. *HIR* and *PAD4* transcripts were expressed in inoculated and control leaves. *EDS1* was only expressed in inoculated leaves, and *SAG101* was not expressed in the RNAseq database (Table 1).

Eight ESTs shared high homology with *HIR* genes, two with *PAD4* genes, and one with *EDS1* gene annotated in *Coffea* spp. genomes (Table 2, *e*-value = 0). Multiple sequence alignments showed that different transcripts of the same *HIR* gene were present (Table 1, Figure S1). For a more effective reference in the text, we named *HIR* genes from 1 to 4 (Table 2) according to the phylogenetic relation with homologs from *Arabidopsis* (Section 3.5).

3.2. Relative Expression of HIR, EDS1 and PAD4 Genes in HDT Leaves along the Infection Process

The transcript profile of the *HIR* gene family and *PAD4* and *EDS1* genes were followed along the infection process under the same experiment layout used to construct the HDT832/2 transcriptome. Three and six time points were chosen: 6 hai, 9 hai and 12 hai for the nonhost interaction with *U. vignae* (U) and 6 hai, 9 hai, 12 hai, 18 hai and 24 hai for the host interaction with *H. vastatrix* (H). Ct values from samples H, U, and control (C) were subject to a prior normalization using Actin-11, Polyubiquitin-like, and Tubulin alpha-2 chain reference genes. The fold change was calculated between the inoculated leaves (U and H) and non-inoculated leaves (C) using the equation depicted in Section 2.5 (Figure 1).

Table 1. Number of reads and relative abundance (Ra) of transcripts with homology to *HIR*, *EDS1* and *PAD4* genes. HDT transcriptome was constructed from leaves inoculated with *Hemileia vastatrix* (H), *Uromyces vignae* (U) and control leaves sprayed with water (C).

Contigs	Reads			Relative Abundance [1]			Gene ID [2]	Gene Name [3]
	H	U	C	H (×1000)	U (×1000)	C (×1000)		
1977	77	192	130	48	119	80	MZ043763	*HIR2;1*
1978	74	187	125	49	125	83	MZ043764	*HIR2;1*
1979	76	190	122	51	127	81	MZ043765	*HIR2;2*
1980	51	32	19	42	26	16	MZ043766	*HIR2;2*
3670	3	3	0	6	6	0	MZ043769	*EDS1*
3754	43	48	10	19	21	4	MZ043770	*PAD4*
3755	43	48	9	19	21	4	MZ043771	*PAD4*
4974	53	29	19	43	24	16	MZ043761	*HIR1*
4975	50	31	18	38	24	14	MZ043762	*HIR1*
9472	52	28	18	40	22	14	MZ043767	*HIR3*
9636	30	50	15	21	35	11	MZ043768	*HIR4*

[1] Ra of transcripts was calculated as the ratio between the number of 454 reads per contig and the length of the assembled contig according to Vega-Arreguín et al. [25]. [2] NCBI ID. [3] Name adopted on the current manuscript.

Table 2. HDT transcripts with homology to *HIR*, *EDS1* and *PAD4* genes mapped on *Coffea arabica*, *C. canephora* and *C. eugenioides* genomes with the depiction of the *e*-value (*E*).

Gene Name *	Gene ID [1]	*Coffea arabica*		*Coffea canephora*		*Coffea eugenioides*	
		E	Gene ID [2] Gene Name *	*E*	Gene ID [3] Gene Name *	*E*	Gene ID [4] Gene Name *
HDTHIR1	MZ043761 MZ043762	0 0	**c-LOC113716961***Ca*$_e$*HIR1* **e-LOC113717595** *Ca*$_c$*HIR1*	0	**Cc11_g13450** *CcHIR1*	0	**LOC113754397** *CeHIR1*
HDTHIR2;1 *HDTHIR2;2*	MZ043763 MZ043764 MZ043765 MZ043766	0 0	**e-LOC113742674** *Ca*$_e$*HIR2* **c-LOC113740361** *Ca*$_c$*HIR2*	0	**Cc04_g15530** *CcHIR2*	0	**LOC113767564** *CeHIR2*
HDTHIR3	MZ043767	0 0	**c-LOC113725125** *Ca*$_e$*HIR3* **e-LOC113730151** *Ca*$_c$*HIR3*	0	**Cc02_g03940** *CcHIR3*	0	**LOC113762209** *CeHIR3*
HDTHIR4	MZ043768	0 0	**c-LOC113700021** *Ca*$_c$*HIR4* **NW_020850478.1-LOC113723124** -	0	**Cc07_g03000** *CcHIR4*	0	**LOC113753487** *CeHIR4*
HDTEDS1	MZ043769	0 0 0	**c-LOC113740411** *Ca*$_c$*EDS1a* **c-LOC113738521** *Ca*$_c$*EDS1b* **e-LOC113742236** *Ca*$_e$*EDS1*	0	**Cc04_g126220** *CcEDS1*	0	**LOC113767316** *CeEDS1*
HDTPAD4	MZ043770 MZ043771	3×10^{-160}	**c-LOC113698404** *Ca*$_c$*PAD4*	0 0	**Cc02_g3389** *CcPAD4a* **Cc02_g3390** *CcPAD4b*	0	**LOC113777610** *CePAD4*

c, chromosome inherited from *C. canephora* parent. **e**, chromosome inherited from *C. eugenioides* parent. [1] NCBI ID. [2] https://www.ncbi.nlm.nih.gov/assembly/GCF_003713225.1 (accessed on 21 November 2022) at NCBI. [3] http://coffee-genome.org/blast (accessed on 21 November 2022) at Coffee genome hub. [4] https://www.ncbi.nlm.nih.gov/assembly/GCF_003713205.1 (accessed on 21 November 2022) at NCBI. * Name adopted on the current manuscript.

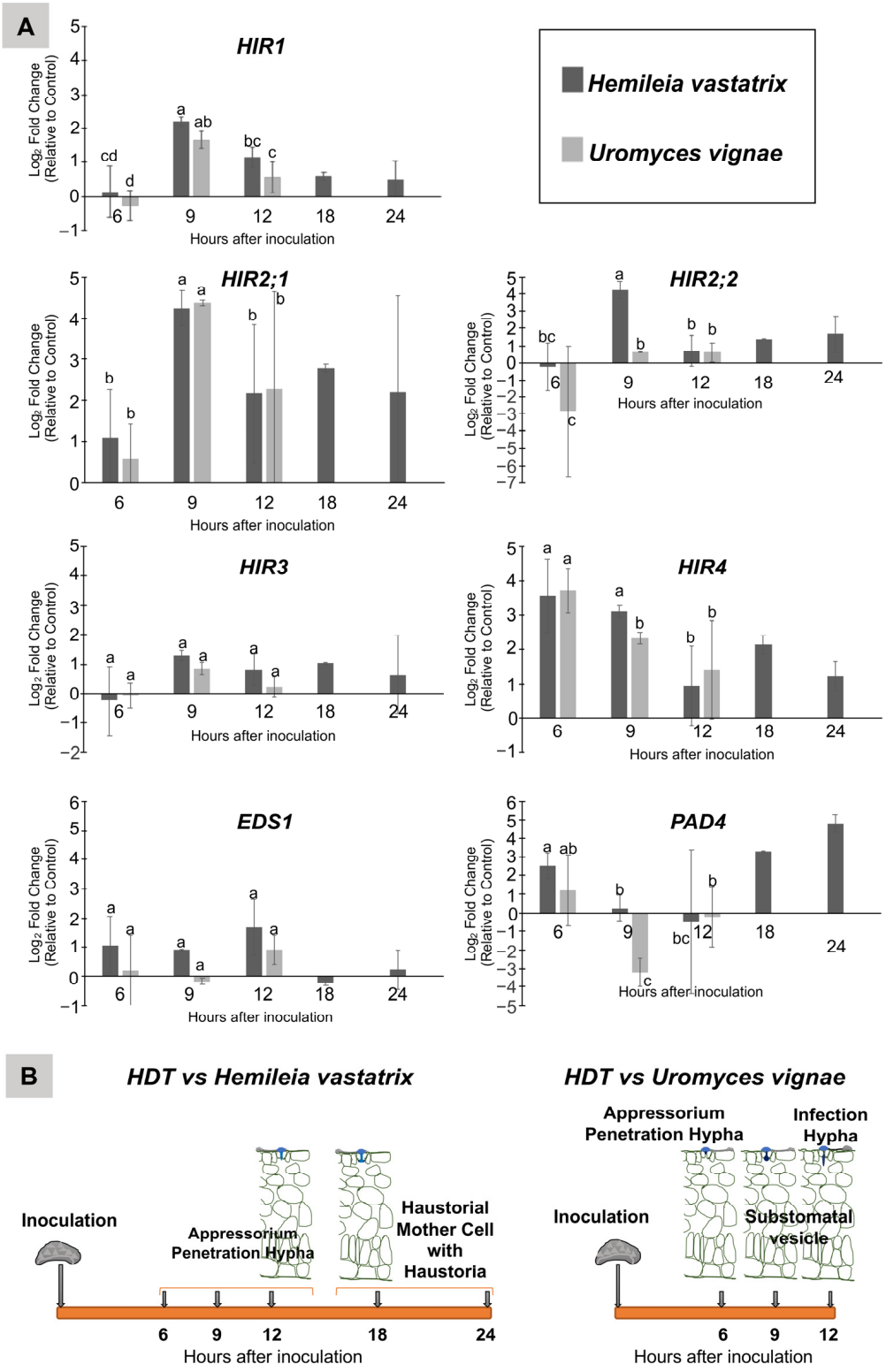

Figure 1. Expression profile of *HIR*, *EDS1* and *PAD4* genes in leaves of HDT inoculated with *Hemileia vastatrix* or *Uromyces vignae*. Fold change was calculated relative to control leaves sprayed with water during leaf infection (**A**). Inoculation was conducted with rust urediniospores. Leaf infection was monitored and sampled 6, 9, 12, 18 and 24 h after inoculation as detailed in the drawings depicted in (**B**), also included is the predominant fungal structure detected in each time-point. Different lower cases indicate significant differences among treatments.

Between 6 hai and 12 hai, *H. vastatrix* differentiated appressoria and penetration hyphae. At 18–24 hai the interaction continued with the production of new fungal structures, such as anchors and a reduced percentage of haustorial mother cells (HMCs) without haustorium. At 6 hai and 12 hai, *U. vignae* produced appressoria, penetration hyphae, substomatal vesicles, and a few infection hyphae, after which the fungal structures started to enter a process of degradation (Figure 1B). Two cytological responses were induced by both rust fungi in HDT leaf cells, HR, and accumulation of phenolic-like compounds in the cytoplasm and in the cell walls. Both were detected earlier in U samples, at 6 hai in 18% of infection sites and 85% at 12 hai, compared with 15% of infection sites in H samples at 12 hai, which increased to 63% of infection sites at 24 hai.

HDTHIR, *HDTEDS1,* and *HDTPAD4* genes were presented in all samples, including the control leaves. The transcript level of the *HDTHIR* gene family (1, 2;1, 2;2, 3 and 4) does not show high levels of regulation in response to rust inoculation except at 9 hai when all members, with the exception of *HDTHIR3*, are upregulated and at 6 hai *HDTHIR4*. As observed for *HDTHIR4*, *HDTPAD4* is upregulated by 6 hai, and *HDTEDS1* was slightly upregulated at 12 hai (Figure 1A).

Summing up, *HDTHIR4* and *HDTPAD4* showed the highest increases in the transcript level early in the infection process (6 hai) in inoculated leaves, but the two genes follow a different profile after that. *HDTHIR4* upregulation progressively diminishes, contrary to *HDTPAD4* fold change that suffers a strong decrease at 9–12 hai, only to increase 18–24 hai in leaves inoculated with coffee rust. Contrarily, three genes from the *HIR* family are the most upregulated ones at 9 hai (Figure 1A). Overall, the upregulation of *HIR* genes in HDT leaves was quite modest, and plant cells probably exert tight control over genes that are reported to be involved in cell death. *EDS1* and *PAD4*, although known to interact with each other, showed a different pattern of fold change. No major differences were observed in the fold change for the chosen genes in host and nonhost interactions in HDT leaves; the only statistically significant difference between the nonhost and host interactions was observed for *HDTHIR2;2*, a two-fold change higher in host interaction at 9 hai.

3.3. Transcript Level of HIR, EDS1 and PAD4 Genes in Coffea arabica Genotypes Involved in Compatible and Incompatible Interactions with Hemileia vastatrix Isolate 178a

Four *C. arabica* genotypes were used to evaluate the variation of the transcript level of *HIR*, *EDS1* and *PAD4* genes during the infection process in leaves inoculated with *H. vastatrix* isolate 178a (race XIV) (Figure 2). *C. arabica* CIFC 19/1 and *C. arabica* CIFC H147/1 genotypes produce a compatible interaction with isolate 178a, and *C. arabica* CIFC 128/2 and *C. arabica* CIFC H469/16 an incompatible one. Four data points were selected representing the evolution of the interactions; 18 hai (0.75) and 1, 2, and 3 days after inoculation (dai). At 18 hai, penetration hyphae were the predominant fungal structure. At 1 dai, HMCs could be observed, and at 2 and 3 dai, HMCs with haustoria were present (Figure 2C).

In the compatible interactions, a faster developmental pace was observed in CIFC 19/1 compared to CIFC H147/1. At 3 dai, the stage of HMC with haustoria was observed in 51% of CIFC 19/1 infection sites compared to 27% in CIFC H147/1. However, by 14 dai, in both interactions, the fungus pursued its growth in about 80% of the infection sites giving rise to macroscopic chloroses and subsequent sporulation. In the incompatible interactions, the fungus reached the stage of HMC with haustoria in 27% of CIFC 128/2 infection sites and 53% in CIFC H469/16, and the fungus ceased to grow beyond this developmental stage in both genotypes. Thus, in CIFC 128/2, the resistance seems to be primarily pre-haustorial, contrary to CIFC H469/16, in which it seems more post-haustorial. In both incompatible interactions, by 14 dai, the first symptoms observed were characterized by reactions type flt (chlorotic fecks with tumefaction).

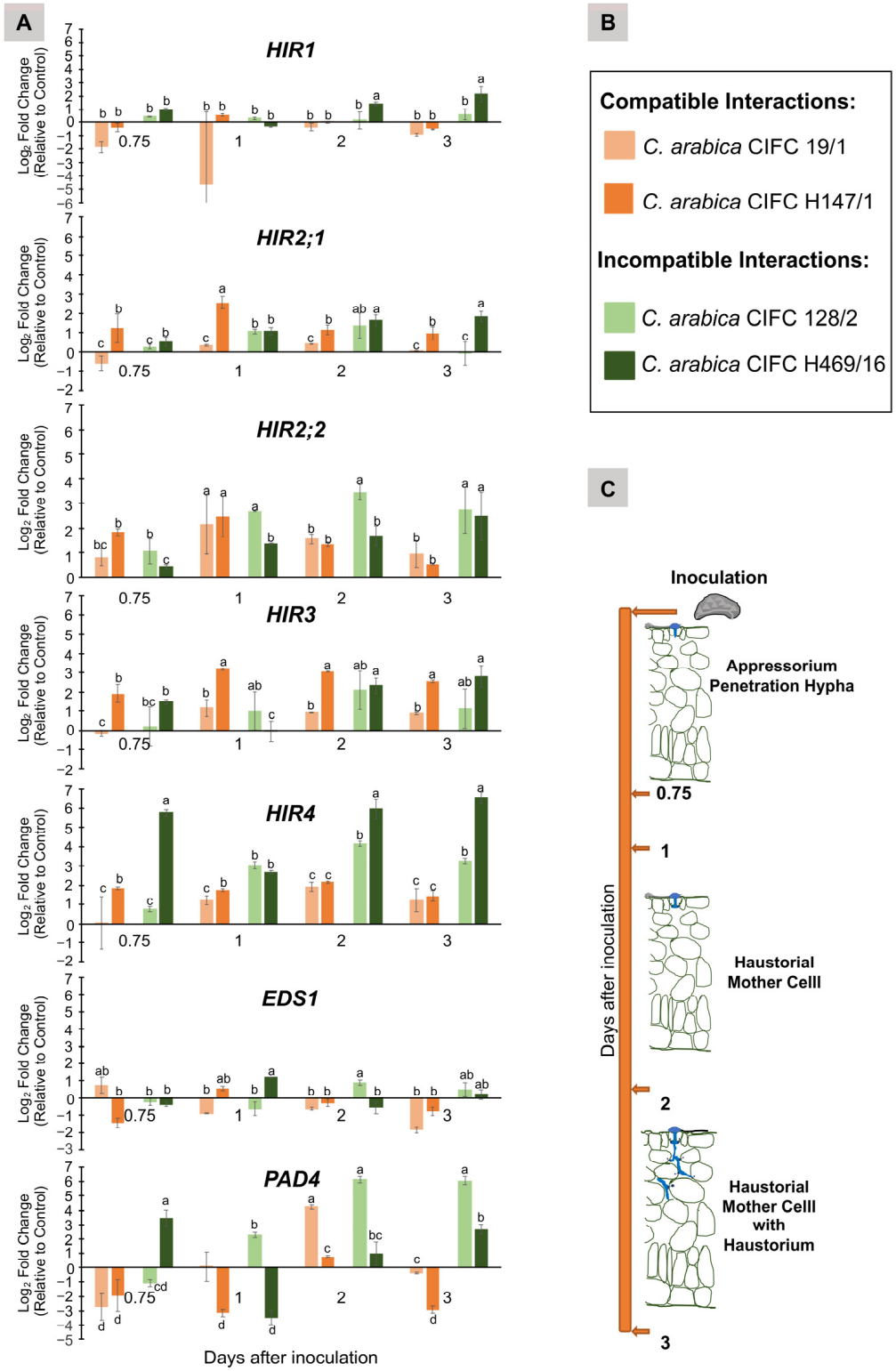

Figure 2. Transcript abundance profile of *HIR*, *EDS1* and *PAD4* genes (**A**) in leaves of *Coffea arabica* genotypes (**B**) inoculated with *Hemileia vastatrix* along the infection process. Transcript abundance was normalized against two reference genes. Inoculation was conducted with *H. vastatrix* urediniospores. Leaf infection was monitored and sampled 0.75, 1, 2 and 3 days after inoculation as detailed in the drawings depicted in (**C**), also included is the predominant fungal structure detected in each time-point. Different lower cases indicate significant differences among treatments.

The fold change was calculated by applying the equation in Section 2.5. The Ct values were normalized using the Ct values of two reference genes, Actin-11 and Tubulin alpha-2 chain, shown to be more stable than the three genes used for normalizing cDNA samples from HDT.

All four *C. arabica* genotypes actively transcribed the *HIR* gene family, *EDS1,* and *PAD4* genes in the data points (Figure 2A). The transcript abundances of *HIR1*, *2;1*, *2;2*, and *3* were about 10 times higher than those of *HIR4* and *EDS1* and 100 times higher than of *PAD4* transcript abundance.

The genotype CIFC H469/16, establishing an incompatible interaction with isolate 178a, showed a fold change increase early in the infection process (peaking at 18 hai), which was especially evident for *HIR4* and *PAD4.* However, the genotype CIFC 128/2, representing an incompatible interaction, did not follow the same pattern (Figure 2A). The early activation in the CIFC H469/16 genotype of *HIR4* and *PAD4* genes is the most noticeable difference between compatible and incompatible interactions.

3.4. Identification of HIR, PAD4 and EDS1 Genes in Coffea Genomes and Relationship with HDT Transcripts

To simplify, we named *C. arabica* genes on the chromosomes originated from the *C. canephora* parent, Ca_c, and originated from the *C. eugenioides* parent, Ca_e.

3.4.1. HIR Gene Family

HIR genes from HDT were used as a query, and BLASTn was the search engine to identify putative *HIR* genes in the genomes of three *Coffea* species. The genes were distributed in three different chromosomes in *C. eugenioides* (chrs. 2, 4 and 11) and in four chromosomes in *C. arabica* and *C. canephora* (chrs. 2, 4, 7 and 11) (Figure 3). The *HIR4* gene was the only gene in which chromosome localization varied between *Coffea* genomes (Figure 3) and was only present in the pool of chromosomes originating from *C. canephora* (Figure 4). A second sequence with high homology to *HDTHIR4* was identified in the *C. arabica* unplaced genomic scaffold, not assigned to a chromosome (NW_020850478.1) (Table 2). This sequence does not have an open reading frame (ORF) and is a probable pseudogene (Table 2). The distinct localization of *HIR4* between the two parent *Coffea* species could be the cause for the loss of a second locus of *HIR4* in the *C. arabica* genome.

HIR1 genes showed that the nucleotide substitutions between *C. arabica* and HDT occurred mainly in the UnTranslated Regions (UTRs) (Figure S1.1). The aa differences in the *HIR1* gene are between homoeologous chromosomes in the *C. arabica* genome.

The alignment of *HIR2* genes shows at the 3′ end, around the predicted stop codon, a nucleotide inclusion of 23 bp in Ca_cHIR2, which incorporated a premature stop codon (TAG). Ca_eHIR2 does not have this sequence and the stop codon (TGA). Curiously this major difference between the two homoeologous genes does not change the protein size but alters the last three aa (SSS instead of EHL, Figure S1.2). Of the four *HDTHIR2* transcripts, two share the protein sequence ending from Ca_cHIR2, and the other two share the one observed in Ca_eHIR2 (Figure S1.2).

The *HIR3* gene shows the lowest number of nucleotide differences between *C. arabica* and HDT, with only one aa substitution in the putative protein sequence (Figure S1.3). Contrarily, the *HIR4* gene was the most diverse gene sequence-wise (Figure S1.4). Its alignment includes sequences from *C. arabica* and both Arabica parents, *C. eugenioides* and *C. canephora*, together with HDT, in order to access which nucleotides are specific to HDT. The *HIR4* gene had 11 nucleotide differences inside CDS; six were responsible for aa variations. *HDTHIR4* had two nucleotides not shared with the other species, which caused two aa modifications (Figure S1.4), making HDTHIR4 a distinct protein sequence.

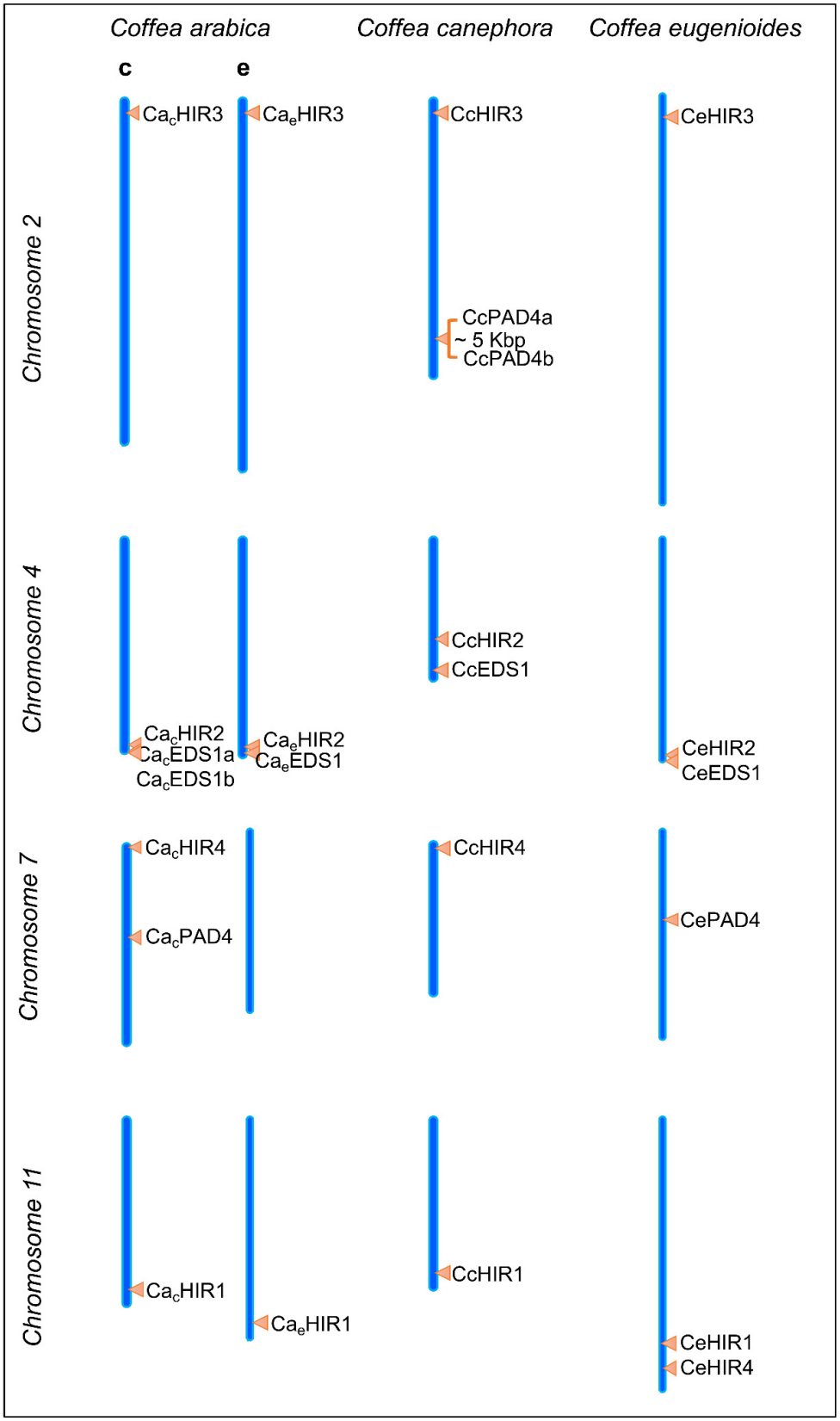

Figure 3. Mapping of *HIR*, *EDS1* and *PAD4* genes on chromosomes of *Coffea arabica*, *C. canephora* and *C. eugenioides* genomes. *C. arabica* genome is divided in chromosomes from the *C. canephora* parent identified with a c, and chromosomes from the *C. eugenioides* parent identified with an e. On top of each chromosome is indicated its number.

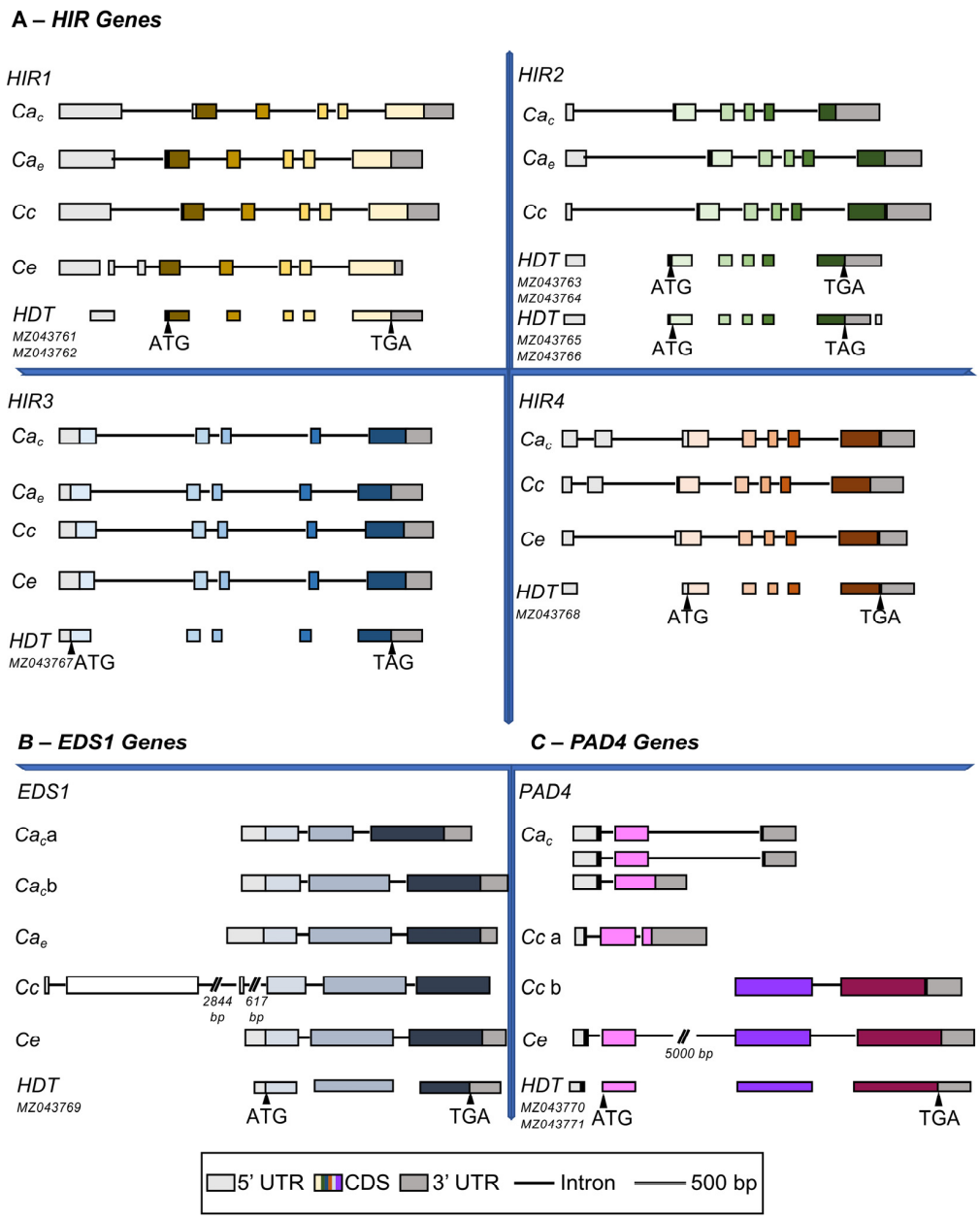

Figure 4. Schematic diagram of the exon–intron structure of *HIR* (**A**), *EDS1* (**B**) and *PAD4* (**C**) genes from *Coffea arabica*, *C. canephora* and *C. eugenioides*. Also included is the representation of the predicted exons from transcripts of the same genes from HDT. Exons are represented by boxes, introns by black lines and untranslated region (UTR) by gray boxes.

A high level of conservation was observed in *HIR* genes between *Coffea* species when considering ORF size, protein length (Table S1), and gene organization (Figure 4). All HIR proteins from *Coffea* spp. contained the characteristic SPFH/Band 7 domain (stomatin/prohibitin/flotillin domain, Pfam01145), which spans almost the entire length of the proteins. This domain is present in prokaryotes and eukaryotes and seems to be localized in cellular membranes [38].

Surprisingly, a portion of *HDTHIR* transcripts share a closer proximity with genes located at the chromosome originating from *C. eugenioides* parent in the *C. arabica* genome or even from the *C. eugenioides* genome, which can be somewhat unexpected considering that HDT is a hybrid between *C. arabica* and *C. canephora*, one would think that the *C. canephora* parent contribution would always be predominant.

3.4.2. EDS1

The *EDS1* gene is located at chromosome four in the *C. arabica* genome and is uniquely duplicated in the chromosome from the *C. canephora* parent. *Ca$_c$EDS1a* and *Ca$_c$EDS1b* share 100% identity and coverage; therefore, they are identical genes located sequentially in the chromosome (Figure 3). Apart from *CcEDS1*, *Coffea EDS1* genes share similar gene size (around 2500 bp), equal protein size (606 aa long), and a parallel gene organization, namely two small introns and three exons (Supplementary Table S1, Figure 4).

HDTEDS1 transcript had an incomplete ORF; specifically, the 3′ end was missing. To obtain a complete ORF, we amplified the *EDS1* gene from leaf cDNA using primers designed on *HDTEDS1* (supplementary file (File S1) primers, HDTEDS1 forward) and on *Ca$_c$EDS1* sequence around the stop codon (LOC113740411, supplementary file (File S1) primers EDS1_Stop). A single band of around 1500 bp was amplified, sequenced, and aligned with *Ca$_c$EDS1* and *HDTEDS1*. The sequence obtained showed a complete ORF that included the partial *HDTEDS1* transcript.

HDTEDS1 seems to be a chimera between Ca$_e$EDS1 and Ca$_c$EDS1; some aa are shared with Ca$_e$EDS1 and CeEDS1, others with Ca$_c$EDS1, and one aa with CcEDS1. We should point out that the sequencing result for *HDTEDS1* detected heterozygosity in some nucleotide positions. The sequence used for putative translation and subsequent analysis was the most frequent one. We cannot discard the possibility that several sequences of *HDTEDS1* are present, such as what we see for *HIR* genes, and the relevance of such variability can be of some importance.

The conserved domains of the EDS1 protein family were predicted in all EDS1 proteins from *Coffea* spp. (Figure 5), namely the Lipase 3 domain (Pfam01764), a characteristic domain of esterases that hydrolyze long-chain acyl-triglycerides, and the Enhanced Disease Susceptibility 1 EP domain (Pfam018117, EDS1_EP). Both domains are located at the C-terminus of EDS1 proteins from *Arabidopsis thaliana* and are responsible for the control of post-infection basal resistance [38]. The EP domain is highly conserved and only found in proteins from this family [20].

CcEDS1 is an unusual gene given that the N-terminus of the predicted protein sequence is constituted by a Formin Homology 2 protein domain (Pfam02181) (Figure 5). This domain is characteristic of Formin (FH) proteins and was never described in EDS1 proteins. The FH protein family control actin rearrangements in the cytoskeleton and its members have been found to interact with Rho-GTPases, profilin, and other actin-associated proteins [39]. Due to the inclusion of this domain, *CcEDS1* is a particularly long gene (7154 bp), with three extra exons and introns (Table S1, Figure 4), and CcEDS1 a larger protein (1071 aa long). However, after the first 464 aa, CcEDS1 is highly homologous to other predicted EDS1 proteins from *Coffea* genotypes (Figure S1.5 and Figure 5).

To check if HDT-inoculated leaves with *H. vastatrix*, *U. vignae,* and/or control leaves were transcribing a gene similar to *CcEDS1,* a set of primers were designed to amplify an *EDS1* gene that would include the Formin domain (supplementary file (File S1) primers: forward EDS1_ATG and reverse HDTEDS1_ATG). However, our attempts were unsuccessful, and the tested cDNA did indicate the presence of an active transcription of an *EDS1* gene with a formin domain. We also were unable to amplify from the cDNA of one genotype of *C. canephora* (CIFC1459) included in CIFC collection and from HDT and *C. canephora* DNA.

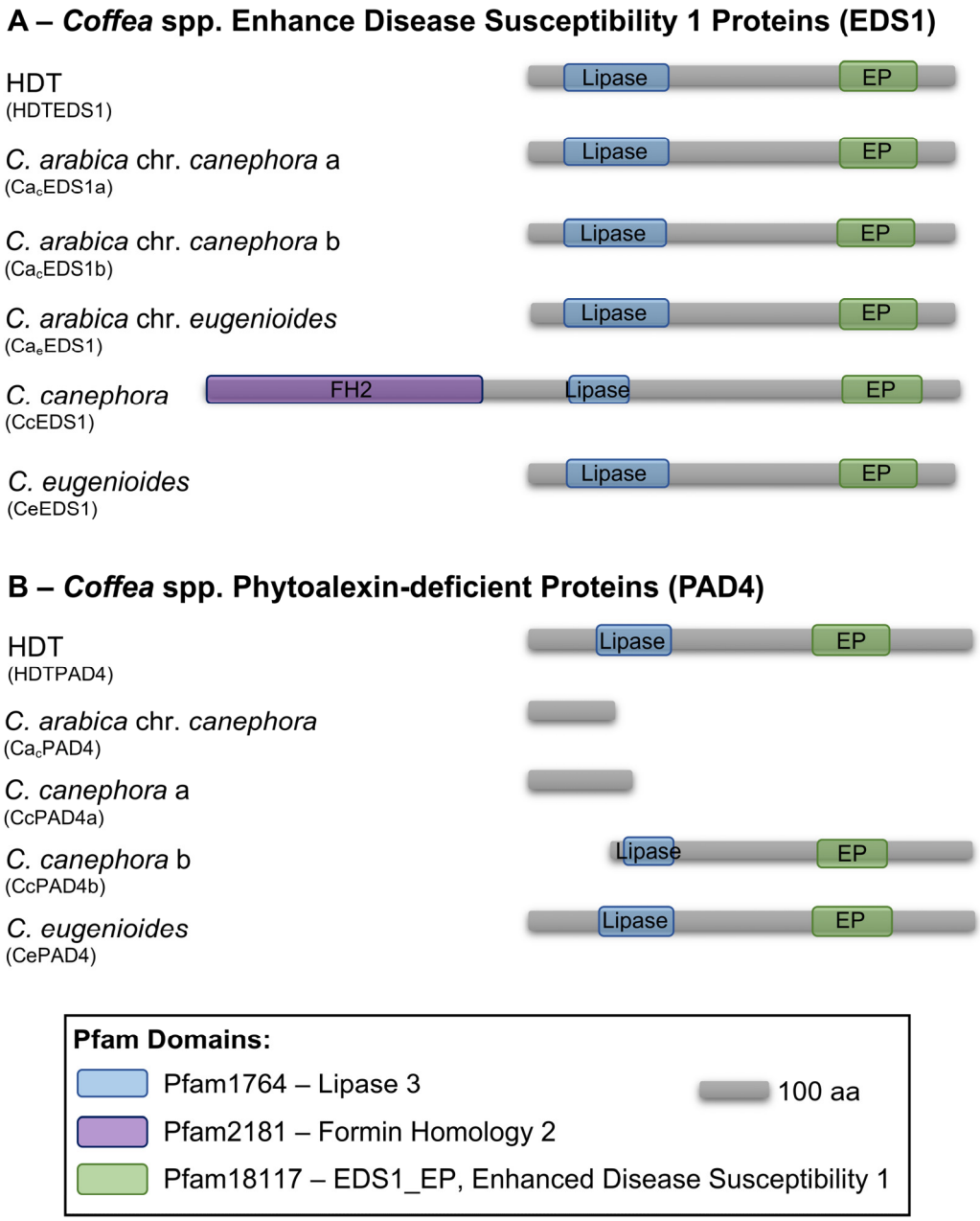

Figure 5. Schematic representation of the conserved domains of EDS1 (**A**) and PAD4 (**B**) proteins in *Coffea* spp. predicted proteins. The conserved motifs identified by screening the Pfam database (http://pfam.xfam.org) (accessed on 2 November 2022) were: Pfam02181, Formin Homology 2; Pfam01764, Lipase 3; Pfam018117, EDS1_EP, Enhanced Disease Susceptibility 1 EP Domain. Protein are represented in gray boxes, and conserved domains in colorful boxes.

3.4.3. PAD4

PAD4 is probably the more diverse gene in this study, considering its chromosome localization, gene organization, and gene and protein sequence (Figures 3–5). In the *C. arabica* genome, one *PAD4* gene is located at chr. 7 (*Ca$_c$PAD4*) and is absent from *C. arabica* chromosomes inherited from the *C. eugenioides* parent. Two genes sharing some homology with *PAD4* (*CcPAD4a* and *CcPAD4b*) are located at chr. 2 in the *C. canephora* genome, and in the *C. eugenioides* genome, one *PAD4* gene is located at chromosome seven (*CePAD4*) (Figure 3).

The two *PAD4* genes in the *C. canephora* genome are separated by 5 kb. Surprisingly, the analysis of the *CePAD4* gene reveals that this 5 kb sequence is partially incorporated as

a second intron, and the 5′ region is highly similar to *Ca$_c$PAD4* and *CcPAD4a*. Contrarily, after the 5 kb intron, the structure and sequence of the gene is like *CcPAD4b*. Consequently, CePAD4 predicted protein seems to be an association of both predicted PAD4 genes from *C. canephora*. The N-terminus shares a high identity with CcPAD4a and Ca$_C$PAD4 proteins, around 120 aa CePAD4 changes to be shared with CcPAD4b (Figure S1.6, Figures 4 and 5).

The two HDT transcripts identified as *PAD4* genes (Table 2) are highly similar to CePAD4, namely in the aa sequence and protein length (Figure S1.6). It is surprising that HDTPAD4 putative proteins (Figure S1.6) have the same structure observed for CePAD4 protein and are different from Ca$_c$PAD4 or CcPAD4 proteins. However, a single modification is caused by a single T deletion in the nucleotide sequence of the *HDTPAD4* transcript (MZ043771), which is shared with the *CcPAD4b* gene sequence, so HDTPAD4 (MZ043771) C-terminus is similar to CcPAD4b, although the protein structure is similar to CePAD4 protein (Figure S1.6).

Ca$_C$PAD4 is similar to *CcPAD4a* (Table S1), though the gene organization is somewhat distinct (Figure 4); *CcPAD4a* has small introns and a large 3′ UTR, and *Ca$_C$PAD4* has three predicted CDS variants, two of each have a quite long intron (Figure 4). Ca$_C$PAD4 and CcPAD4a proteins are not predicted to have any of the two conserved domains of PAD4 proteins (Figure 5). Contrarily, CcPAD4b, CePAD4, and HDTPAD4 protein sequences showed the typical domains of PAD4 proteins (Figure 5).

The PAD4 gene has major differences between *Coffea* species, namely in the gene and protein structure. It would be interesting to study the lack of both domains in the protein function.

3.5. Phylogenetic Analysis of HIR Genes in Coffea spp. and Arabidopsis

A. thaliana HIR protein family has been studied in detail, and some of their members have been functionally characterized (e.g., [12]). We conducted a phylogenetic analysis between HIR proteins from *Arabidopsis thaliana* and *Coffea* spp. in an effort to create an association between them and gain insight into the function of HIR proteins from *Coffea* spp.

The phylogenetic tree was inferred using the maximum likelihood method based on the alignment of HIR protein sequences. The tree with the highest log likelihood shows that AtHIR1 protein clusters with a set of *Coffea* HIR (named HIR1) and AtHIR3 clusters with a different set of *Coffea* HIR (named HIR3). A separate branch subdivided into two separate groups of *Coffea* protein sequences distinguished between HIR2 and HIR4. However, their association with AtHIR2 and AtHIR4 was not direct (Figure 6A). A more straightforward association was observed between CcHIR and the Ca$_c$HIR proteins and CeHIR and the Ca$_e$HIR proteins (Figure 6A), as expected, corroborating the origin of the chromosomes in the *C. arabica* genome.

HDTHIR2;2 is 100% identical to CacHIR2 and CcHIR2, and HDTHIR2;1 to CaeHIR2 and CeHIR2, which means that HDTHIR2 is actively transcribed in both homoeologous chromosomes (Figure 6A and Figures S1.1–S4).

HIR3 proteins are the most distinct HIR group showing a clearer separation from the rest (Figure 6A). However, the protein alignment shows large segments with high homology between sequences, in particular at the SPFH/Band 7 domain. This domain is implicated in the HIR protein's capacity to form heterocomplexes [12] (Figure 6B).

The MEME algorithm was used to search for new conserved motifs in HIR proteins, which could reflect the different clusters in HIR proteins depicted in the phylogenetic tree. Seven conserved domains were detected with e-values ranging from 2.9×10^{-1026} to 9.3×10^{-13} (Figures 6B and S2). Four are inside the SPFH/Band 7 domain, and three are, one at the N-terminus and two at the C-terminus. All motifs with significant *e*-values are shared by the sequences, except one that includes the first methionine and is specific to HIR3 proteins (Figures 6B and S2).

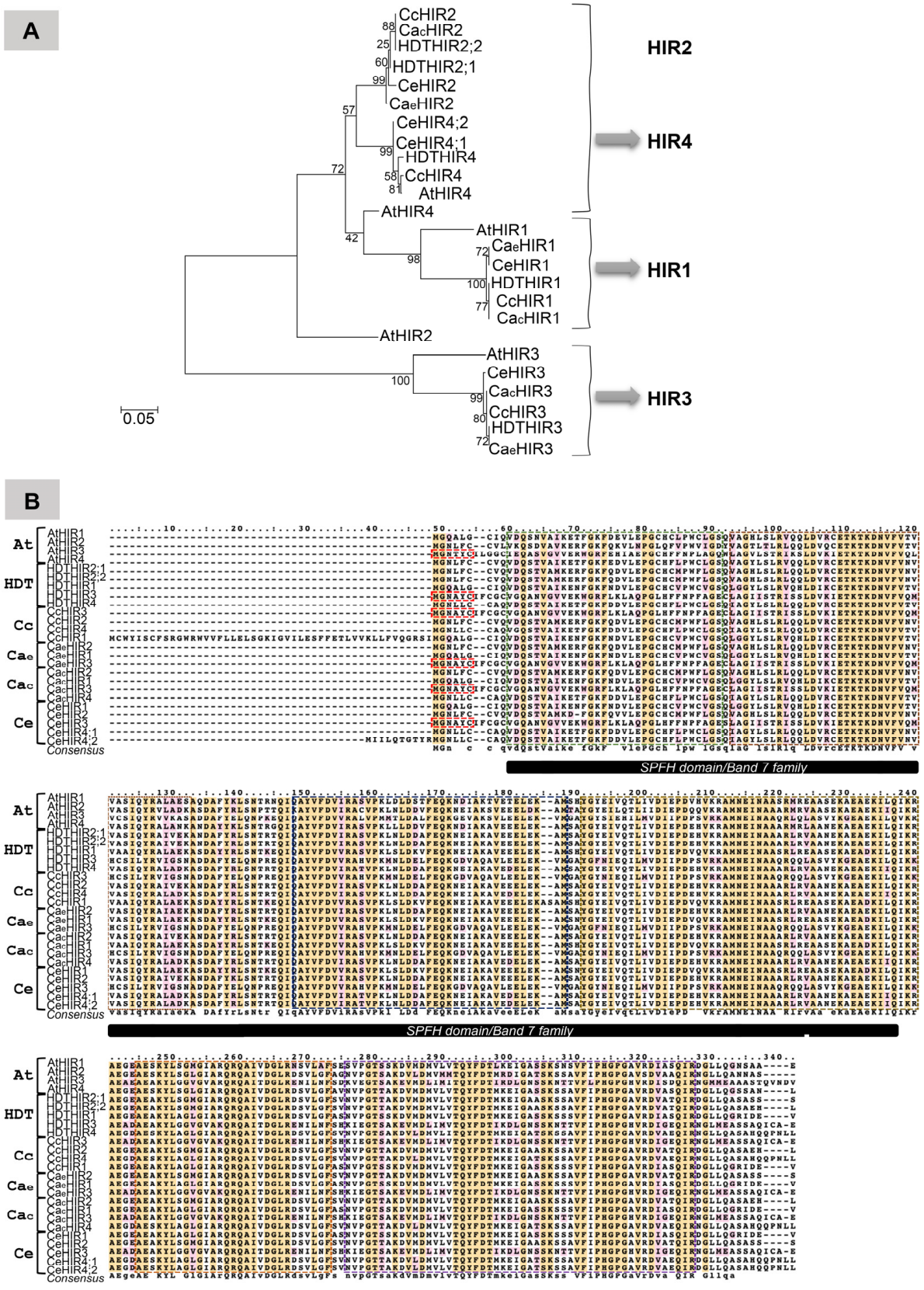

Figure 6. (**A**) Phylogenetic tree of putative HIR proteins from *Arabidopsis thaliana* (At), *Coffea arabica* (Ca), *C. canephora* (Cc), *C. eugenioides* (Ce) and *Coffea* Timor hybrid (HDT). The tree was drawn to scale and constructed using the maximum likelihood method conducted in software MEGA7. (**B**). Amino acid sequence alignment of HIR proteins from *Arabidopsis thaliana* (At), *Coffea arabica* (Ca),

Coffea canephora (Cc), *Coffea eugenioides* (Ce) and *Coffea* HDT. The multiple sequence alignment was carried out using the T-coffee server (http://tcoffee.crg.cat/apps/tcoffee/do:mcoffee) (accessed on 16 November 2022) and visualized with the pyBoxShade program (https://github.com/mdbaron42/pyBoxshade/releases) (accessed 20 March 2023) with the depiction of the consensus sequence. Amino acid residues with an orange background are the same in all sequences and with a pink background are similar to the consensus sequence. The conserved SPFH/Band 7 domain (stomatin/prohibitin/flotillin domain, Pfam01145) predicted at Pfam server (http://pfam.xfam.orgis) (accessed on 11 November 2022) is indicated under the sequences in a black box. Colored boxed regions are conserved domains predicted at MEME suite (https://meme-suite.org/meme/) (accessed on 18 October 2022) for detailed information see Figure S2. Protein sequence IDs are included in Supplementary File S1.

Some characteristics of AtHIR proteins are not predicted for *Coffea* spp. sequences, namely the presence of transmembrane domains (using http://www.cbs.dtu.dk/services/TMHMM/algorithm) (accessed on 10 October 2022) or the glycine myristoylation near the first methionine (Figure 6B, using https://web.expasy.org/myristoylator/) (accessed on 17 October 2022).

3.6. Phylogenetic Analysis of EDS1 and PAD4 Proteins

EDS1 and PAD4 proteins have been characterized as important components of plant immunity to pathogens (e.g., [18]). The phylogenetic relationship between EDS1 and PAD4 *Coffea* spp. proteins and a select group of plant species were inferred using the maximum-likelihood method [19]. EDS1 and PAD4 orthologs were identified in sequenced plant genomes from different plant families, namely the Poaceae, Brassicaceae, and Solanaceae [20].

EDS1 and PAD4 protein sequences can be used to design a unique tree due to their high degree of conservation. Such a tree was added as supplementary data (Figure S3), and individual trees were constructed for EDS1 and PAD4 sequences (Figure 7). The reduced size of PAD4 sequences from *C. arabica* (Ca_cPAD4) and *C. canephora* (CcPAD4a) (Figure S1.6), and the PAD4 sequences with shorter N-terminus from *C. canephora* (CcPAD4b), *Populus trichocarpa* and *Erythranthe guttata*, made it difficult to align all PAD4 proteins and impaired the analysis conducted by the MEGA7 software. Therefore, three phylogenetic trees with a better score were drawn (Figure 7).

Minor differences were observed in the species distribution and structure in all the trees (Figure 7). EDS1 and PAD4 protein sequences from *Coffea* spp., as excepted, formed a tight cluster, as the species from the Poaceae and Brassicaceae. Proteins from *Musa acuminata* joined the Poaceae cluster probably because it is a monocot species. EDS1 and PAD4 protein sequences from *Solanum tuberosum* and *E. guttata* are distributed near the *Coffea* sequences since they all belong to the Asterids clade, contrary to the rest of the Eudicots species used that belong to the Rosids clade or in the case of *Aquilegia coerulea* to the core Eudicots clade (Figure 7).

EDS1 and PAD4 proteins have an N-terminus homologous to lipase proteins, an α/β hydrolase fold lipase incorporating in a Serine(S)-Aspartic Acid (D)-Histidine (H) catalytic triad. The catalytic triad S-D-H has been proven essential to the lipase activity, but more importantly appears to facilitate the binding between EDS1 and PAD4 [20], which is necessary for full capacity for basal resistance [19].

The S-D-H triad was present in all *Coffea* EDS1 proteins, and the GHSSG motif was fully conserved. The aa around D and H in EDS1 changed accordingly with *C. eugenioides* or *C. canephora* origin, and HDTEDS1 shares the aa with the *C. canephora* parent (Figure 7B). PAD4 proteins also have the catalytic triad, again quite conserved between *Coffea* sequences; GH***S***VG, QH***D***IV, and ED***H***LN. However, Ca_cPAD4 and CcPAD4a are shorter proteins without the lipase or EP domains (Figure 5); consequently, the catalytic triad is also missing. *C arabica* genome does not appear to have a second PAD4 gene near the identified PAD4 gene, such as what we observed in the C. *canephora* genome or in a different chromosome.

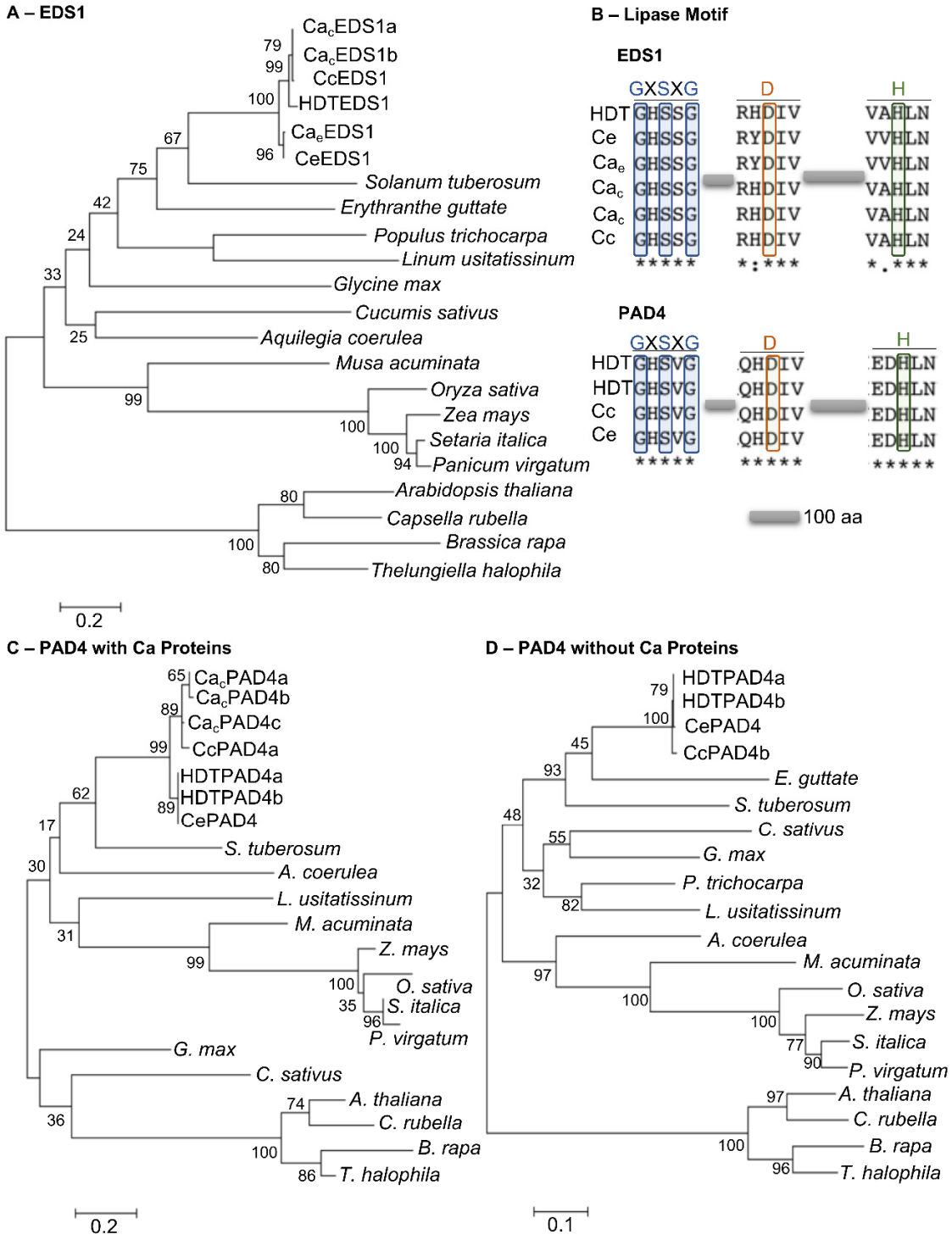

Figure 7. (**A**). Phylogenetic tree of putative EDS1 proteins from *Coffea arabica* (Ca), *C. canephora* (Cc), *C. eugenioides* (Ce), *Coffea* Timor hybrid (HDT) and a selected group of orthologs sequences. (**B**). Conservation of lipase catalytic triad residues in EDS1 and PAD4 *Coffea* spp. sequences aligned with T-Coffee. Conserved positions within the catalytic S-D-H of α/β hydrolases, namely the GxSxG motif, are shown. (**C**). Phylogenetic tree of putative PAD4 proteins from *C. arabica* (Ca), *C. canephora* (Cc), *C. eugenioides* (Ce), *Coffea* Timor hybrid (HDT) and a selected group of orthologs sequences. (**D**). Phylogenetic tree of putative PAD4 proteins from *C. canephora* (Cc), *C. eugenioides* (Ce), *C.* Timor hybrid (HDT) and a selected group of orthologs sequences. All trees were drawn to scale and constructed using the maximum likelihood method conducted in software MEGA7. Protein sequence IDs are included in Supplementary File S1. * Conserved amino acids.

3.7. PAD4 Gene Structure in Selected Coffea Genotypes

The *PAD4* gene revealed striking differences between *Coffea* genomes that can have direct consequences in their resistance profile. We conducted an analysis to predict if the genomic area where the PAD4 gene is inserted is similar to the parent *C. canephora* or the parent *C. eugenioides* in four *C. arabica* genotypes that were used in the qPCR experiments and whose genome sequence is not known.

All individuals showed that the percentage of paired reads with both ends mapping on the same contig was always higher at the contig belonging to the *C. canephora* genome (Table 3). The average mapping quality at the contig from the *C. canephora* genome ranged between 56.99 and 58.11. Such values were consistently higher than those found at the contig from the *C. eugenioides* genome (51.27–53.89, Table 2). Finally, at all individuals, the average distance between mapping locations of paired ends showed values consistent with that of the insert at the contig from the *C. canephora* genome (487–549 bp) in contrast to the higher distances found at the contig from the *C. eugenioides* genome (2614–10,706 bp). This genomic analysis points to the *PAD4* gene in all four genotypes being more like the structure found in *C. canephora*, with two individual *PAD4* genes and not one *PAD4* with a long first intron.

Table 3. Affinity of paired-end reads to target contigs of *Coffea canephora* and *C. eugenioides*. Mapping quality and distance between paired ends shows average and 95% CI ranges.

C. arabica Genotype	Paired-Read Ends Mapped on the Same Contig (%)		Mapping Quality (q)		Distance between Paired Ends (bp)	
	C. canephora	*C. eugenioides*	*C. canephora*	*C. eugenioides*	*C. canephora*	*C. eugenioides*
19/1	61.34	45.47	57.56 (40–60)	53.37 (28–60)	549 (59–2051)	10,706 (117–10,798)
128/8	60.38	24.61	57.62 (40–60)	52.86 (27–60)	514 (59–1068)	7453 (89–10,809)
H147/1	62	27.31	57.69 (40–60)	53.54 (27–60)	510 (59–1062)	8646 (112–10,797)
H469	59.42	53.88	57.63 (40–60)	53.89 (27–60)	549 (59–1064)	10,706 (114–10,798)

4. Discussion

The importance of HDT as a source of resistance against several diseases affecting coffee plants cannot be understated. Within the HDT population, it is possible to find plants resistant to diseases caused by fungi, such as *H. vastatrix* and *Colletotrichum kahawae*, by the nematode *Meloidogyne exigua*, or by the bacterium *Pseudomonas syringae* pv. *garcae* [2,6]. Amongst HDT accessions, CIFC 832/2 continues to be of much interest. Occasional reports of broken resistance to coffee leaf rust have been described in some coffee-growing countries, such as India. Remarkably, one hundred years after the discovery of HDT at Timor Island, the molecular nature of its broad-range resistance remains a mystery. The analysis of HDT CIFC 832/2 transcriptome was conducted to shed light on what contributes to its basal resistance.

The *HIR* gene family, *EDS1* and *PAD4*, were present in the RNAseq database from inoculated leaves of HDT with *H. vastatrix* or *U. vignae* and are implicated in several processes related to plant immunity. The RT-qPCR analysis sustained the presence of the genes in the transcriptome.

HIR4 and *PAD4* were the genes with the greatest transcript fold change in inoculated HDT leaves with both rust species compared to non-inoculated leaves. The same two genes showed a greater fold change in the initial stage (18 hai) of the infection in the incompatible interaction between *C. arabica* CIFC H469/16 and *H. vastatrix* isolate 178a. The upregulation of *HIR* genes has been documented before in wheat when infected with rust [14,15] in *Nicotiana benthamiana*, and *Oryza sativa* infected with the rice stripe virus [17], and also in response to bacterial PAMPs in *Arabidopsis thaliana* [12]. It is interesting to note that *HIR4* and *PAD4* genes, together with *EDS1*, had the lower transcript abundance of all the genes studied, suggesting a tight and sensible control of the genes that have been linked to cell death HR, which can be detrimental when occurring without purpose. These three genes

also showed a higher variation: in chromosome localization (*HIR4* and *PAD4*); at the level of gene and protein sequence (all three); and *EDS1* is subject to one duplication event.

No major differences were observed in the fold change of the genes studied in response to *H. vastatrix* or *U. vignae*; likewise, no major differences were detected in the cytological observations made previously [7], contributing to the idea that the distinction between host and nonhost resistance response is blurry and even that nonhost resistance can be a confusing concept in functional terms as suggested by [11].

There is a lack of coherence between the gene response and the type of interaction in which the *C. arabica* genotypes are engaged. For example, *C. arabica* 128/2 inoculated with 178a seems to have a transcript pattern closer to the other compatible genotypes, which in turn do not coincide between them. *PAD4* gene transcript level could be seen as a good example that one of the incompatible interactions is more pre-haustorial (CIFC 128/2), and the other is more post-haustorial (CIFC H469/16). However, it does not justify completely such a different response in the transcript level of the *PAD4* gene since we observed that the *PAD4* gene is upregulated in HDT leaves in response to *H. vastatrix*, which are engaged in a strong pre-haustorial resistance [7], and in *U. vignae*, which is completely pre-haustorial. Consequently, the coffee genotype CIFC 128/2 is probably employing other strategies and weapons in the fight against *H. vastatrix*.

The *PAD4* gene structure in each genotype can also be responsible for its less important role. The restricted analysis that we performed showed that the *PAD4* gene in all genotypes was more conserved with the structure of the gene in the C. *canephora* genome. Thus, a complementary analysis of the *PAD4* gene sequence in a number of coffee genotypes would be revealing since significant differences could be detected and could play a more important role in this context.

The availability of three annotated genomes of *Coffea* species, Arabica, and its parents permitted us to characterize in detail the *HIR* gene family, *EDS1* and *PAD4* genes, and furthermore compared it with the sequences in HDT transcriptome. *Coffea* genomes, as expected, revealed similar gene localization on the chromosomes between species, with the exception of *HIR4* and *PAD4* genes. Interestingly, in the *C. arabica* genome, both genes were lost in the chromosomes from the *C. eugenioides* parent. Since *CeHIR4* is located at the 3′ end of chromosome 11 in *C. eugenioides* and chromosome 11 from *C. arabica* is shorter, which could result in an erroneous resolution of chromosome 11 end and/or a flawed chromosome 11e assembly.

The loss of the Ca_ePAD4 gene probably has a distinct explanation. Chromosome seven, where *PAD4* is located in the genome sequencing of *C. arabica* var. Bourbon, was subjected to a drastic reorganization [40]. The 1.2-Mbp terminal of this chromosome suffered a replacement of *C. canephora* DNA with *C. eugenioides* DNA. This homoeologous replacement caused this region of chromosome seven to have four copies of *C. eugenioides* DNA. The authors suggest that this replacement occurred immediately after the unique hybridization event that originated *C. arabica.* Consequently, the available genome from *C. arabica* var. Caturra Red would also reflect the same homoeologous replacement. The fact that PAD4 is located at chromosome seven, like in the genome of *C. eugenioides*, and not at chromosome two as observed in the C. *canephora* genome, seems to confirm that the replacement with *C. eugenioides* DNA also occurred in *C. arabica* var. Caturra Red. However, it does not explain everything, namely the missing *PAD4* gene on the chromosome from *C. eugenioides* in the *C. arabica* var. Caturra Red genome. Therefore, other drastic chromosome rearrangements must have occurred.

Coffea HIR proteins were quite conserved between isoforms, in particular, the characteristic SPFH responsible for guaranteeing the localization of *Capsicum annuum* HIR protein in microdomains along the plasma membrane [41]. However, contrary to other HIR proteins [12,41], there was no prediction of canonical transmembrane domains for *Coffea* HIRs. The new conserved protein domains found by the MEME algorithm in all *Coffea* spp. and *A. thaliana* proteins could be involved in this localization to microdomains

in membranes since they spanned throughout the SPFH domain, or help in the constitution heteroligomer protein complexes.

Recently, HIR1 from tomatoes was identified as a target of an effector from the Tomato leaf curl Yunnan virus. This interaction interfered with HIR's capacity for self-interaction and compromised HR reaction [42]. In 2011 Choi et al. [41] suggested that the protein microdomains could function as sites for effector detection or delivery. The existence of different HIR isoforms, all expressed in HDT transcriptome, and in the case of HDTHIR2, both homoeologous proteins, may provide a way of diversifying and escaping effector detection and protecting HR.

EDS1, PAD4, and SAG101 proteins share the lipase and the EP conserved domains and produce heterocomplexes [43]. The *SAG101* gene was not identified in our RNAseq database, but it is present in *C. arabica, C. canephora,* and *C. eugenioides* genomes. The *PAD4* gene in the *Coffea* spp. genome and *EDS1* in the C. *canephora* genome revealed major surprises. *C. arabica* genome does not have a *PAD4* gene containing a predicted EP domain or lipase domain. *C. canephora* genome has one gene with homology to *EDS1,* and its putative translation has a predicted Formin FH2 domain, which is not typically found in the EDS1/PAD4/SAG101 gene family.

EDS1 and PAD4 protein association is a weak one, dependent on the EP domain and strengthen by the lipase domain [19]. The functional EDS1/PAD4 protein complex leads to the upregulation of *PAD4* transcripts and the mobilization of the SA pathway [43,44]. Concomitantly, *A. thaliana* plants expressing a mutated EDS1 unable to interact with PAD4 were compromised in their basal resistance to avirulent bacteria, but EDS1 and PAD4 independently were able to trigger HR at the infection site [19]. However, *A. thaliana* plants expressing a PAD4 incapable of interacting with AtEDS1, since it contained only the lipase domain, did not trigger basal resistance or ETI [43]. Our experimental data indicate that the absence of both protein domains in CaPAD4 makes it impossible to interact with the EDS1 protein; therefore, *C. arabica* var. Caturra Red's capability for basal resistance should be quite diminished. Actually, this genotype is known for its high susceptibility to diseases [2].

We could not amplify an *EDS1* transcript from the cDNA of HDT and *C. canephora* leaves or from the DNA of both species that includes a Formin FH2 domain, which made us suspicious of the *EDS1 C. canephora* genome annotation. However, a BLASTp search reveals two genes: one from *Vitis vinifera* (unnamed protein product, sequence ID CBI15099.3) and another from *Citrus sinensis* (protein eds1-related, sequence ID KAH9719992.1), with *EDS1* genes that included a predicted FH2, lipase and EP domains with varying sizes. *Vitis vinifera*, like *C. arabica*, has several *EDS1* genes [45,46], contrary to *C. canephora* and *C. eugenioides* genomes, which only have one predicted *EDS1* gene.

We can speculate that the mechanism behind the *CcEDS1* could be similar to the one suggested for the *PAD4* gene in *C. eugenioides* and HDT. The fusion of two independent genes and an intergenic region transformed in an intron. In the *C. arabica* and *C. eugenioides* genomes, the genes flanking *EDS1* are always formin-8-like genes, which reinforces the hypothesis of gene fusion. However, *C. arabica* genome chr. *canephora* does not show the *C. canephora* version of the EDS1 protein. Thus a hypothetical fusion had to have occurred after the hybridization event that originated *C. arabica*. Still, the phylogenetic analysis shows that CcEDS1 clusters tightly with both EDS1 proteins present in the *C. arabica* genome (Ca_cEDS1a and Ca_cEDS1b), even if with a different N-terminus.

We did not test all the *C. canephora* genotypes available in germplasm collections nor the genotype used for sequencing, but in our limited analysis, we could not confirm the inclusion of the formin-8 domain in CcEDS1. However, it is curious that in other species, such an EDS1 protein is also predicted. However, it is difficult to predict the impact on EDS1 function if the mature protein contained a Formin FH2 domain. Does it change the subcellular localization of EDS1? In *Arabidopsis*, the EDS1 pool in the cytoplasm and the nucleus directly impacted basal and TIR-NLR immunity [47]. Liu and colleagues [48] showed that restricting EDS1 in the cytoplasm decreases the resistance capacity. Or is EDS1

able to interact with PAD4 or SAG101 proteins? As mentioned before, these interactions are important in the overall resistance response.

Furthermore, a Formin FH2 domain included in the mature EDS1 protein is a gain? The FH2 domain is a conserved domain of Formin 8 proteins which are involved in the nucleation of actin filaments [49] and localized at the cell membrane in the contact point with other cells [50]. Actin is proposed to play a role in the interaction between the extracellular space and intercellular signaling necessary to activate plant defenses and to be involved in the regulation of transcription [51]. EDS1 and PAD4 proteins are known to be transcriptional inducers of genes in the SA pathway [18]. Recently it was shown by chromatin immunoprecipitation assay that EDS1 protein can bind to the promoter of isochorismate synthase one gene, directly upregulating its transcription [52].

HIR, EDS1, and PAD4 proteins are directly involved in the fulfillment of plant immunity. *EDS1* and *PAD4* genes are of special interest since they are good targets for improving the resistance potential [43], but they can also influence drought tolerance and increase biomass production, as observed in *Populus* [53,54]. EDS1 and PAD4 genes, and their protein complex, have been functionally characterized in *Arabidopsis* and *Nicotiana.* The unexcepted gene structure uncovered in the *PAD4* gene from *C. arabica* or EDS1 from *C. canephora* needs to be further explored to characterize the real impact that the different structures of the genes may have in the capacity for basal resistance and TIR-NLR drive immunity.

Considering the low diversity observed in both wild and cultivated varieties of *C. arabica* due to a suggested species bottleneck [40], the search for variability has to be conducted outside *C. arabica* species. The study of HDT is of special interest because hybrid species, in general, can combine favorable characteristics from different parents and/or reveal new traits. The fact that HDT is already a stable tetraploid and can be crossed with *C. arabica* varieties with good commercial characteristics is also an advantage, making the crossing with *C. arabica* less prone to deleterious effects.

5. Conclusions

The present study revealed that, amongst the genes studied, *HIR4* and *PAD4* genes showed a transcription upregulation early in the infection process of *Hemileia vastatrix* and *Uromyces vignae* on leaves of Timor hybrid (HDT 832/2- *Coffea arabica* × *C. canephora*) (host vs. nonhost resistance), and of *H. vastatrix* on *C. arabica* CIFC H469/16 leaves (host resistance). The transcription patterns of the *HIR* gene family, *PAD4*, and *EDS1* genes did not differ between the nonhost and host resistance responses in HDT leaves. Moreover, *HIR4*, *PAD4*, and *EDS1* genes showed the highest sequence diversity in *C. arabica*, *C. canephora*, and *C. eugenioides* genomes. The predicted proteins of PAD4 in *C. arabica* and EDS1 in *C. canephora* are atypical proteins within the PAD4/EDS1 protein family, the first lacks all the conserved domains and the second has a protein domain named formin. These differences in the amino acid sequences could alter the protein function and impact the resistance responses. Further in-depth research is needed to decipher the complexity of the coffee resistance processes, a piece of crucial knowledge for developing efficient disease resistance breeding.

Supplementary Materials: The following supporting information can be downloaded at: https://www.mdpi.com/article/10.3390/agronomy13040992/s1, Figure S1. Multiple sequence alignment of HIR1, HIR2, HIR3, HIR4, EDS1 and PAD4 genes of *Coffea* ssp. Alignments were carried out using T-coffee server (http://tcoffee.crg.cat) (accessed on 16 November 2022). Nucleotide and amino acid differences are encircled by orange boxes, the first ATG by a yellow box and the STOP codon by a blue box. Figure S2. A. Motifs identified by the MEME algorithm (https://meme-suite.org/meme/) (accessed on 18 October 2022) using complete amino acids sequences of 25 HIR genes from *Coffea* spp. and *Arabidopsis thaliana*. Motifs are numbered according with their position in the protein sequences. B. Distribution of the conserved motifs identified in MEME algorithm in a scheme representing a generic HIR protein. Different motifs are indicated by different collors and numbered 1 to 7 corresponding to the numbers in the table above. Figure S3. Phylogenetic analysis of putative *Coffea*

spp. EDS1 and PAD4 with AtEDS1 and AtPAD4 and orthologs from a select group of species. Table S1. List of HIR, EDS1 and PAD4 genes identified in *Coffea arabica*, *Coffea canephora*, *Coffea eugenioides* genomes and HDT transcriptome and their corresponding gene, open reading frame (ORF) and protein size. File S1: List of primers and Sequences ID.

Author Contributions: Conceptualization, S.T.; writing—original draft preparation, S.T., H.A., M.d.C.S. and P.T.; writing—review and editing, S.T., H.A., M.d.C.S. and P.T.; methodology, S.T., H.A., M.d.C.S., P.T., J.V. and A.J.M.-P. All authors have read and agreed to the published version of the manuscript.

Funding: This research was co-funded by Foundation for Science and Technology (FCT) and FEDER funds through PORNorte under the project CoffeeRES ref. PTDC/ASP-PLA/29779/2017, and by FCT UNIT LEAF (UID/AGR/04129/2020).

Data Availability Statement: Not applicable.

Conflicts of Interest: The authors declare no conflict of interest.

References

1. Maghuly, F.; Jankowicz-Cieslak, J.; Souleymane, B. Improving coffee species for pathogen resistance. *CAB Rev.* **2020**, *15*. [CrossRef]
2. Silva, M.d.C.; Guerra-Guimarães, L.; Diniz, I.; Loureiro, A.; Azinheira, H.; Pereira, A.P.; Tavares, S.; Batista, D.; Várzea, V. An overview of the mechanisms involved in coffee-*Hemileia vastatrix* interactions: Plant and Pathogen Perspectives. *Agronomy* **2022**, *12*, 326. [CrossRef]
3. Cressy, D. Coffee rust regains foothold. researchers marshal technology in bid to thwart fungal outbreak in Central America. *Nature* **2013**, *493*, 587.
4. Sieff, K. The migration problem is a coffee problem. *Washington Post*, 2019.
5. Bettencourt, A.J.; Rodrigues, C.J. Principles and practice of coffee breeding for resistance to rust and other diseases. *Coffee Agron.* **1988**, *4*, 199–234.
6. Silva, R.A.; Zambolim, L.; Castro, I.S.L.; Rodrigues, H.S.; Cruz, C.D.; Caixeta, E.T. The Híbrido de Timor germplasm: Identification of molecular diversity and resistance sources to coffee berry disease and leaf rust. *Euphytica* **2018**, *214*, 153. [CrossRef]
7. Diniz, I.; Talhinhas, P.; Azinheira, H.G.; Várzea, V.; Medeira, C.; Maia, I.; Petitot, A.S.; Nicole, M.; Fernandez, D.; Silva, M.C. Cellular and molecular analyses of coffee resistance to *Hemileia vastatrix* and nonhost resistance to *Uromyces vignae* in the resistance-donor genotype HDT832/2. *Eur. J. Plant Pathol.* **2012**, *133*, 141–157. [CrossRef]
8. Talhinhas, P.; Batista, D.; Diniz, I.; Vieira, A.; Silva, D.N.; Loureiro, A.; Tavares, S.; Pereira, A.P.; Azinheira, H.G.; Guerra-Guimarães, L.; et al. The coffee leaf rust pathogen *Hemileia vastatrix*: One and a half centuries around the tropics. *Mol. Plant Pathol.* **2017**, *18*, 1039–1051. [CrossRef]
9. Yu, X.; Feng, B.; He, P.; Shan, L. From chaos to harmony: Responses and signaling upon microbial pattern recognition. *Annu. Rev. Phytopathol.* **2017**, *55*, 109–137. [CrossRef]
10. Monteiro, F.; Nishimura, M.T. Structural, functional, and genomic diversity of plant NLR proteins: An evolved resource for rational engineering of plant immunity. *Annu. Rev. Phytopathol.* **2018**, *56*, 243–267. [CrossRef]
11. Panstruga, R.; Moscou, M.J. What is the molecular basis of nonhost resistance? *Mol. Plant Microbe Interact.* **2020**, *33*, 1253–1264. [CrossRef] [PubMed]
12. Qi, Y.; Tsuda, K.; Nguyen, L.V.; Wang, X.; Lin, J.; Murphy, A.S.; Glazebrook, J.; Thordal-Christensen, H.; Katagiri, F. Physical association of Arabidopsis hypersensitive induced reaction proteins (HIRs) with the immune receptor RPS2. *J. Biol. Chem.* **2011**, *286*, 1297–1307. [CrossRef] [PubMed]
13. Karrer, E.E.; Beachy, R.N.; Holt, C.A. Cloning of tobacco genes that elicit the hypersensitive response. *Plant Mol. Biol.* **1998**, *36*, 681–690. [CrossRef] [PubMed]
14. Duan, Y.; Guo, J.; Shi, X.; Guan, X.; Liu, F.; Bai, P.; Huang, L.; Kang, Z. Wheat hypersensitive-induced reaction genes *TaHIR1* and *TaHIR3* are involved in response to stripe rust fungus infection and abiotic stresses. *Plant Cell Rep.* **2013**, *32*, 273–283. [CrossRef]
15. Yu, X.-M.; Zhao, W.-Q.; Yang, W.-X.; Liu, F.; Chen, J.-P.; Goyer, C.; Liu, D.-Q. Characterization of a Hypersensitive Response-Induced gene *TaHIR3* from wheat leaves infected with leaf rust. *Plant Mol. Biol. Rep.* **2012**, *31*, 314–322. [CrossRef]
16. Rostoks, N.; Schmierer, D.; Kudrna, D.; Kleinhofs, A. Barley putative hypersensitive induced reaction genes: Genetic mapping, sequence analyses and differential expression in disease lesion mimic mutants. *Theor. Appl. Genet.* **2003**, *107*, 1094–1101. [CrossRef]
17. Li, S.; Zhao, J.; Zhai, Y.; Yuan, Q.; Zhang, H.; Wu, X.; Lu, Y.; Peng, J.; Sun, Z.; Lin, L.; et al. The Hypersensitive Induced Reaction 3 (HIR3) Gene Contributes to Plant Basal Resistance via an EDS1 and Salicylic Acid-Dependent Pathway. *Plant J.* **2019**, *98*, 783–797. [CrossRef]
18. Dongus, J.A.; Parker, J.E. EDS1 signalling: At the nexus of intracellular and surface receptor immunity. *Curr. Opin. Plant Biol.* **2021**, *62*, 102039. [CrossRef]
19. Rietz, S.; Stamm, A.; Malonek, S.; Wagner, S.; Becker, D.; Medina-Escobar, N.; Vlot, A.C.; Feys, B.J.; Niefind, K.; Parker, J.E. Different roles of enhanced disease susceptibility 1 (EDS1) bound to and dissociated from phytoalexin deficient 4 (PAD4) in Arabidopsis immunity. *New Phytol.* **2011**, *191*, 107–119. [CrossRef]

20. Wagner, S.; Stuttmann, J.; Rietz, S.; Guerois, R.; Brunstein, E.; Bautor, J.; Niefind, K.; Parker, J.E. Structural basis for signaling by exclusive EDS1 heteromeric complexes with SAG101 or PAD4 in plant innate immunity. *Cell Host Microbe* **2013**, *14*, 619–630. [CrossRef]
21. Denoeud, F.; Carretero-Paulet, L.; Dereeper, A.; Droc, G.; Guyot, R.; Pietrella, M.; Zheng, C.; Alberti, A.; Anthony, F.; Aprea, G. The coffee genome provides insight into the convergent evolution of caffeine biosynthesis. *Science* **2014**, *345*, 1181–1184. [CrossRef] [PubMed]
22. Loureiro, A.; Azinheira, H.G.; Silva, M.C.; Talhinhas, P. A method for obtaining RNA from *Hemileia vastatrix* appressoria produced in planta, suitable for transcriptomic analyses. *Fungal Biol.* **2015**, *119*, 1093–1099. [CrossRef] [PubMed]
23. Silva, M.C.; Nicole, M.; Rijo, L.; Geiger, J.P.; Rodrigues, C.J., Jr. Cytochemical aspects of the plant-rust fungus interface during the compatible interaction *Coffea arabica* (cv. Caturra)-*Hemileia vastatrix* (race III). *Int. J. Plant Sci.* **1999**, *160*, 79–91. [CrossRef]
24. Silva, M.C.; Nicole, M.; Guerra-Guimarães, L.; Rodrigues, C.J. Hypersensitive cell death and post-haustorial defence responses arrest the orange rust (*Hemileia vastatrix*) growth in resistant coffee leaves. *Physiol. Mol. Plant Pathol.* **2002**, *60*, 169–183. [CrossRef]
25. Vega-Arreguín, J.C.; Ibarra-Laclette, E.; Jiménez-Moraila, B.; Martínez, O.; Vielle-Calzada, J.P.; Herrera-Estrella, L.; Herrera-Estrella, A. Deep Sampling of the Palomero Maize Transcriptome by a High Throughput Strategy of Pyrosequencing. *BMC Genom.* **2009**, *10*, 299. [CrossRef]
26. Sambrook, J.; Russell, D.W. *Molecular Cloning: A Laboratory Manual*; Cold Spring Harbor Laboratory: Cold Spring Harbor, NY, USA, 2001.
27. Xie, F.; Xiao, P.; Chen, D.; Xu, L.; Zhang, B. miRDeepFinder: A miRNA analysis tool for deep sequencing of plant small RNAs. *Plant Mol. Biol.* **2012**, *80*, 75–84. [CrossRef]
28. Ramakers, C.M.; Ruijter, J.; Lekanne Deprez, R.H.; Moorman, A.F.M. Assumption-free analysis of quantitative real-time polymerase chain reaction (PCR) data. *Neurosci. Lett.* **2003**, *339*, 62–66. [CrossRef]
29. Pfaffl, M.W. A new mathematical model for relative quantification in real-time RT-PCR. *Nucleic Acids Res.* **2001**, *29*, e45. [CrossRef]
30. Notredame, C.; Higgins, D.G.; Heringa, J. T-coffee: A novel method for fast and accurate multiple sequence alignment. *J. Mol. Biol.* **2000**, *302*, 205–217. [CrossRef]
31. Marchler-Bauer, A.; Bo, Y.; Han, L.; He, J.; Lanczycki, C.J.; Lu, S.; Chitsaz, F.; Derbyshire, M.K.; Geer, R.C.; Gonzales, N.R.; et al. CDD/SPARCLE: Functional classification of proteins via subfamily domain architectures. *Nucleic Acids Res.* **2017**, *45*, D200–D203. [CrossRef]
32. Käll, L.; Krogh, A.; Sonnhammer, E.L.L. Advantages of combined transmembrane topology and signal peptide prediction-the Phobius web server. *Nucleic Acids Res.* **2007**, *35*, W429–W432. [CrossRef] [PubMed]
33. Bailey, T.L.; Boden, M.; Buske, F.A.; Frith, M.; Grant, C.E.; Clementi, L.; Ren, J.; Li, W.W.; Noble, W.S. MEME Suite: Tools for motif discovery and searching. *Nucleic Acids Res.* **2009**, *37*, W202–W208. [CrossRef] [PubMed]
34. Jones, D.T.; Taylor, W.R.; Thornton, J.M. The rapid generation of mutation data matrices from protein sequences. *Comput. Appl. Biosci.* **1992**, *8*, 275–282. [CrossRef] [PubMed]
35. Kumar, S.; Stecher, G.; Tamura, K. MEGA7: Molecular evolutionary genetics analysis version 7.0 for bigger datasets. *Mol. Biol. Evol.* **2016**, *33*, 1870–1874. [CrossRef]
36. Martin, M. Cutadapt removes adapter sequences from high-throughput sequencing reads. *EMBnet J.* **2011**, *17*, 10–12. [CrossRef]
37. Li, H.; Durbin, R. Fast and Accurate Short Read Alignment with Burrows-Wheeler Transform. *Bioinformatics* **2009**, *25*, 1754–1760. [CrossRef]
38. Rivera-Milla, E.; Stuermer, C.A.; Malaga-Trillo, E. Ancient origin of reggie (flotillin), reggie-like, and other lipid-raft proteins: Convergent evolution of the SPFH domain. *Cell. Mol. Life Sci.* **2006**, *63*, 343–357. [CrossRef]
39. Blanchoin, L.; Staiger, C.J. Plant formins: Diverse isoforms and unique molecular mechanism. *Biochim. Biophys. Acta* **2010**, *1803*, 201–206. [CrossRef]
40. Scalabrin, S.; Toniutti, L.; Gaspero, G.; Scaglione, D.; Magris, G.; Vidotto, M.; Pinosio, S.; Cattonaro, F.; Magni, F.; Jurman, I.; et al. A single polyploidization event at the origin of the tetraploid genome of *Coffea arabica* is responsible for the extremely low genetic variation in wild and cultivated germplasm. *Sci. Rep.* **2020**, *10*, 4642. [CrossRef]
41. Choi, H.W.; Kim, Y.J.; Hwang, B.K. The hypersensitive induced reaction and leucine-rich repeat proteins regulate plant cell death associated with disease and plant immunity. *Mol. Plant-Microbe Interact.* **2011**, *24*, 68–78. [CrossRef]
42. Mei, Y.; Ma, Z.; Wang, Y.; Zhou, X. Geminivirus C4 antagonizes the HIR1-mediated hypersensitive response by inhibiting the HIR1 self-interaction and promoting degradation of the protein. *New Phytol.* **2020**, *225*, 1311–1326. [CrossRef] [PubMed]
43. Bhandari, D.D.; Lapin, D.; Kracher, B.; von Born, P.; Bautor, J.; Niefind, K.; Parker, J.E. An EDS1 heterodimer signalling surface enforces timely reprogramming of immunity genes in Arabidopsis. *Nat. Commun.* **2019**, *10*, 772. [CrossRef]
44. Cui, H.; Gobbato, E.; Kracher, B.; Qiu, J.; Bautor, J.; Parker, J.E. A core function of EDS1 with PAD4 is to protect the salicylic acid defense sector in Arabidopsis immunity. *New Phytol.* **2017**, *213*, 1802–1817. [CrossRef]
45. Gao, F.; Shu, X.; Ali, M.B.; Howard, S.; Li, N.; Winterhagen, P.; Qiu, W.; Gassmann, W. A functional EDS1 ortholog is differentially regulated in powdery mildew resistant and susceptible grapevines and complements an Arabidopsis eds1 mutant. *Planta* **2010**, *231*, 1037–1047. [CrossRef] [PubMed]
46. Gao, F.; Dai, R.; Pike, S.M.; Qiu, W.; Gassmann, W. Functions of EDS1-like and PAD4 genes in grapevine defenses against powdery mildew. *Plant Mol. Biol.* **2014**, *86*, 381–393. [CrossRef] [PubMed]

47. Garcia, A.V.; Blanvillain-Baufume, S.; Huibers, R.P.; Wiermer, M.; Li, G.; Gobbato, E.; Rietz, S.; Parker, J.E. Balanced nuclear and cytoplasmic activities of EDS1 are required for a complete plant innate immune response. *PLoS Pathog.* **2010**, *6*, e1000970. [CrossRef]
48. Liu, H.; Li, Y.; Hu, Y.; Yang, Y.; Zhang, W.; He, M.; Li, X.; Zhang, C.; Kong, F.; Liu, X.; et al. EDS1-interacting J protein 1 is an essential negative regulator of plant innate immunity in Arabidopsis. *Plant Cell* **2021**, *33*, 153–171. [CrossRef]
49. Yi, K.; Guo, C.; Chen, D.; Zhao, B.; Yang, B.; Ren, H. Cloning and functional characterization of a formin-like protein (AtFH8) from Arabidopsis. *Plant Physiol.* **2005**, *138*, 1071–1082. [CrossRef]
50. Deeks, M.J.; Cvrčková, F.; Machesky, L.M.; Mikitová, V.; Ketelaar, T.; Žárský, V.; Davies, B.; Hussey, P.J. Arabidopsis group Ie formins localize to specific cell membrane domains, interact with actin-binding proteins and cause defects in cell expansion upon aberrant expression. *New Phytol.* **2005**, *168*, 529–540. [CrossRef]
51. Porter, K.; Day, B. From filaments to function: The role of the plant actin cytoskeleton in pathogen perception, signaling and immunity. *J. Integr. Plant Biol.* **2016**, *58*, 299–311. [CrossRef]
52. Lapin, D.; Bhandari, D.D.; Parker, J.E. Origins and immunity networking functions of EDS1 family proteins. *Annu. Rev. Phytopathol.* **2020**, *58*, 253–276. [CrossRef] [PubMed]
53. Bernacki, M.J.; Czarnocka, W.; Szechynska-Hebda, M.; Mittler, R.; Karpinski, S. Biotechnological potential of LSD1, EDS1, and PAD4 in the improvement of crops and industrial plants. *Plants* **2019**, *8*, 290. [CrossRef] [PubMed]
54. Szechyńska-Hebda, M.; Czarnocka, W.; Hebda, M.; Bernacki, M.J.; Karpiński, S. PAD4, LSD1 and EDS1 regulate drought tolerance, plant biomass production, and cell wall properties. *Plant Cell Rep.* **2016**, *35*, 527–539. [CrossRef] [PubMed]